

Pricing and Risk in Sovereign Green Debt: Evidence from Chile*

Lautaro Chittaro[†] Marcelo Sena[‡]
(Job Market Paper)

November 6, 2025
[link to latest version]

Abstract

We study the pricing of sovereign green bonds using Chile's pioneering green bond program and its cross-design issuance. Employing a panel of Chilean U.S.-dollar bonds, we estimate no-arbitrage pricing kernels for green and conventional bonds. The results reveal a declining greenium across maturities, driven by the higher interest-rate risk exposure of green bonds. We find no evidence of investor segmentation or liquidity differences between green and conventional bonds. Instead, we explain the observed pricing patterns through a representative-agent asset-pricing model in which investors derive nonpecuniary benefits from the real value of their green bond holdings. During high-inflation periods, as observed in our sample, the real value of green bond portfolios deteriorates, making the convenience service they provide scarcer and more valuable. This positive correlation between green convenience yield and inflation generates a risk premium that compresses the greenium especially at longer maturities, producing a downward-sloping greenium term structure.

*We are especially grateful to Monika Piazzesi and Martin Schneider for their continuous guidance, support and encouragement. We would also like to thank Hanno Lustig, Luigi Bocola, Adrien Auclert, Angus Lewis, Oliver Xie, Arvind Krishnamurthy, Chris Tonetti and Bård Harstad for helpful comments and suggestions. This research was supported by the Stanford Woods Institute for the Environment Emerging Environmental Scholar Award, the George P. Schultz Dissertation Support Fund and the Gale and Steve Kohlhagen Fellowship in Economics. Some of the computing for this project was performed on the Sherlock cluster. We would like to thank Stanford University and the Stanford Research Computing Center for providing computational resources and support that contributed to these research results. All errors are our own.

[†]Stanford University

[‡]Stanford University, msena@stanford.edu

1. Introduction

The market for sovereign green bonds, debt instruments directed toward green projects, has expanded rapidly in recent years. Existing work documents a modest and positive greenium, the yield differential between conventional and green bonds, often attributing it to a static convenience yield arising from investor taste. This presents an opportunity to finance environmental projects at a discount. However overlooks a critical dimension typically under control of issuers, how the greenium behaves across different maturities. If the value investors place on green assets fluctuates with macroeconomic conditions, this should create a non-trivial term structure of greenia, a possibility that remains largely unexplored. In this case the greenium reflects not only average convenience but also compensation for bearing that risk. Treating the greenium as a constant convenience yield may mismeasure issuance costs across maturities by overlooking important risk exposures.

This paper presents facts and theory for the term structure of greenia for Chilean sovereign bonds, a pioneer in green bond issuance. We show that Chile's sovereign greenium is largest at short maturities and declines with maturity. This downward slope reflects not only differences in expected future greenium, but, importantly, different priced risk. Liquidity or investor segmentation does not explain this differential pricing. Instead, we rationalize it through a representative-investor model with preferences over real (inflation-adjusted) green bond portfolio. In states of high inflation, as in our sample, green convenience becomes scarce and therefore more valuable; this positive correlation commands a risk premium that depresses the greenium especially at long maturities.

We find a greenium, the yield differential between a conventional and a green bond, for a 5-year bond of 20 basis points (bps), which declines monotonically to zero at the 20 year maturity. Our empirical setting leverages Chile's U.S.-dollar-denominated sovereign green bond program, which provides variation for green and conventional bonds at different maturities over time. The measurement strategy estimates a no-arbitrage, exponentially affine term structure model that prices these green and conventional coupon bonds. This structure allows us to decompose each yield into a path of short rates and compensation for loading on risk factors; estimating it jointly for green and conventional bonds allows us to recover this same decomposition for the greenium.

A no-arbitrage term structure model is important because green and conventional bonds are not directly comparable as they differ in maturity. Raw yield differences do not properly account for term-premia. To overcome this, we estimate a green and conventional stochastic discount factor (SDF) that prices the respective bonds. We pool the full cross-section and time series and impose common macro-financial factors that drive the dynamics of the SDFs.

Allowing separate affine SDFs for green and conventional bonds does not violate no-arbitrage because it is observationally equivalent to a single representative-investor kernel with an

asset-specific, nonpecuniary service flow (convenience yield) attached to green holdings. Our joint estimation imposes the same macro-financial state vector across both term structures and interprets the wedge between both SDFs as a stochastic convenience yield process. Our estimation recovers a persistent and negative comovement of this convenience yield with the investors' SDF. This negative correlation is a risk premium component that shapes the slope of the greenium curve.

We rule out that our SDF differences is driven by segmented green bond investors. Using fixed-income holdings data we show that for a panel of funds holding at least one Chilean sovereign bond, more than 50% of these funds held both a green and conventional bond. Similarly, we also rule out liquidity drives our results. Bid-ask spreads of green and conventional bonds are similar.

Theoretically, we show that green preferences typically used in climate finance models imply a different risk exposure for green bonds when accounting for sources of macroeconomic risk. We provide a general decomposition of the greenium term structure, in which the key driver is the covariance between the investor's stochastic discount factor and a stochastic convenience yield driven by taste for green assets. Given the prominence of inflation as a risk factor in our sample, we model investors' green convenience as the real value of the green portfolio.

A parsimonious calibration with inflation being the only source of risk can generate a downward sloping greenium term structure, explaining 15% of the empirical slope. The mechanism is as follows: high inflation erodes the real value of green wealth, leading to high marginal convenience. Because the nominal SDF typically moves inversely with inflation, convenience is high precisely when the nominal SDF is low; the convenience-SDF covariance is negative, which raises required returns on green bonds and reduces the greenium.

Long maturities bear a larger convenience-risk penalty because the covariance stacks over time and is amplified by persistence. A one-year bond only has a short stream of risky convenience flows, while a 10-year bond prices the entire stream of future convenience flows. Persistence in inflation makes the effect stronger: an inflation shock that raises convenience (in real terms) today tends to keep convenience high while the nominal SDF stays low for several years, amplifying risk premia in longer maturity bonds.

A natural question is why any green-conventional price difference would survive arbitrage. The naive trade, short the expensive green bond and go long the cheap conventional bond, does not deliver a riskless profit in our setting. Because maturities and coupons differ, the position loads on term-premium, duration, and convexity risk. A riskless profit is only obtained if the strategy is carried until maturity of the bonds. Further, mark-to-market fluctuations may create funding and margin call risk. Trading frictions are also likely to bite: shorting specific green bonds can be difficult given limited lendable supply and buy-and-hold ESG investors. As documented in Section 4, bid–ask spreads are on the order of 10–20 bps for both conventional and

green bonds are an order of magnitude larger than typical highly liquid benchmarks. Together, risk, funding constraints, and transaction costs make it plausible that the price differences we document are not fully eliminated.

One natural concern with our findings is why such price differences, in particular a cheaper conventional bond, would persist in the markets. An investor without any green preference could potentially arbitrage the difference by short-selling the expensive green bond. There are a couple of reasons why this strategy might not be feasible in practice. First, even in the absence of any trading costs, this strategy would not be riskless, since it would only lead to a sure profit if held to maturity. In particular, the market value of such a strategy would fluctuate solely due to changes in term-premia, since green and conventional bonds in our sample have different maturities. Also, trading and shorting costs for these green bonds are likely to be high. For example, as we show in section 4, bid-ask spreads are of the order of 10-20bps for both conventional and green bonds, which is an order of magnitude larger than a typical liquid bond whose bid-ask spread is typically 1bp in the worst case. Hence, both trading costs and the presence of risk are likely to be important market forces that prevent systematic differences between green and conventional bond prices to be eliminated.

These results have direct issuance and policy implications. Short maturity sovereign green debt appears materially cheaper but carries a different risk profile, so maturity choice trades off lower interest rates against greater exposure to interest-rate risk specific to green bonds. The magnitudes are meaningful: a 20 bps savings between issuing at five versus twenty years is about \$66 million per year, roughly 1% of Chile's annual budget deficit. Our framework lets sovereigns and investors evaluate such trade-offs and different green bond designs, supporting more cost-effective financing while advancing environmental goals.

As an application, we use the estimated SDFs to value alternative instruments and to size their financial incentives. We leverage Chile's pioneering sustainability-linked bonds (SLBs) issuance, a novel bond design whose coupons step up if environmental targets are missed. We show they price much like standard green bonds, suggesting investors reward credible green signaling, even though these bonds do not allocate proceeds to specific green projects. We further quantify the market value of the coupon step-ups, to gauge the size of environmental incentives in these bonds. Discounting shrinks the financial bite of step-ups: the annualized financing cost implied by a potential step-up is roughly one fifth of the headline number; for example, a 50 bps potential step-up translates to roughly 8-10 bps in effective annual costs.

Related literature. Our paper develops a no-arbitrage term-structure model for sovereign green bonds and uses it to measure the maturity profile of the greenium, the difference between the interest rates on conventional and green bonds. We build on an empirical literature that typically finds small green premia but uses different identification strategies across markets ([Giglio](#),

[Kelly and Stroebel \(2021\)](#), [Hong and Shore \(2023\)](#)). For stocks, [Bolton and Kacperczyk \(2021\)](#) document the existence of a carbon premium in the US stock market, consistent with exclusionary screening. [Pástor, Stambaugh and Taylor \(2022\)](#) show that green stocks outperformed brown stocks recently, but that expected returns going forward are lower for green stocks. [Pedersen et al. \(2021\)](#) estimates an efficient frontier when incorporating environmental, social and governance (ESG) factors, finding an empirically small cost for tilting the portfolio towards low carbon stocks. [Engle et al. \(2020\)](#) show how to construct portfolios that hedge climate news, finding it performs effectively out-of-sample. [Ilhan et al. \(2021\)](#) measures a higher cost to protect from downside tail risk in option markets for carbon intensive firms. [Bauer et al. \(2025\)](#) show that brown stocks are more negatively affected by tighter monetary policy. [Gormsen, Huber and Oh \(2024\)](#) document that green firms perceive their cost of capital to be lower, which incentivizing allocation of resources toward greener investment. Our main sample of Chilean green bonds are similarly of the use-of-proceeds type which imposes contractual obligations for investment in green projects; we show they are indeed priced with a smaller yield. [Berk and Van Binsbergen \(2025\)](#) finds that divestment strategies do not produce meaningful cost of capital changes, suggesting directed investment and corporate control are likely to be more effective. The design of use-of-proceeds bonds we study are a step in this direction, where funds are directed toward specific projects. Finally, [Hong and Kacperczyk \(2009\)](#) show that expected returns for “sin” stocks (related to alcohol, tobacco, and gambling) is higher and that are less held by norm-constrained institutions like pension funds. Overall, these papers show that ESG concerns is consequential for the pricing and risk in stock prices. We show the same is true for green bonds for both short and long maturity green bonds.

On bonds, the quantitative estimates of the greenium are mixed, but most evidence points to a modest but positive greenium. [Baker, Bergstresser, Serafeim and Wurgler \(2018\)](#) document a greenium for U.S. municipals and corporates green bonds and interpret it through investor nonpecuniary utility; we take the same taste channel to the sovereign term-structure and show how such a theory implies different risk-exposure for green and conventional bonds that finds support in the data through our estimated no-arbitrage model. [Pástor, Stambaugh and Taylor \(2022\)](#) show how realized green bond returns can be high during a transition phase, in which investors develop green tastes and start buying green assets, implying that simple averages can mislead about expected premia. We also measure state dependent green returns, showing how it can vary with inflation risk. [Zerbib \(2019\)](#) estimates a greenium of 2bp while [Larcker and Watts \(2020\)](#) argue that once risk and contractual features are controlled for the greenium is near zero. Our baseline estimate finds greenium that is relatively larger for Chilean sovereign green bonds, of around 20 bps for a 5 year bond, but declining in maturity, with no statistically significant greenium beyond the 10 year maturity. Our estimate of the greenium below 5 year maturity admittedly noisy due to the lack of green bonds with less than 5 year maturity in our sample.

This is generally true for the broader universe of green bonds, which are typically issued at longer horizons. For this reason, our finding of declining greenium with maturity is not only the more robust fact but also more empirically relevant. In line with our findings, [Fatica, Panzica and Rancan \(2021\)](#) find a greenium for supranationals and corporates; [Caramichael and Rapp \(2024\)](#) show an issuance premium for U.S./euro corporate green bonds. [Flammer \(2021\)](#) documents real effects around corporate green issuance. The magnitude of the greenium in these papers serves as external discipline on the magnitude of the greenia our model recovers. We build on them by showing how imposing additional structure, through the exponentially-affine form for stochastic discount factor for estimation, allows us to measure greenia across comparable but not identical sets of securities.

A growing body of work targets sovereign green bonds specifically. [Roch, Ando, Fu and Wiriadinata \(2023\)](#) provide a broad cross-country assessment of sovereign greenium magnitudes, smaller in advanced economies and larger in emerging markets. We complement their cross-sectional lens with a structural time-series approach that recovers maturity-specific sovereign green premia. Twin-bond programs, most prominently Germany's, create near-perfect green/conventional comparisons and an observable green yield curve at multiple maturities. [Pástor et al. \(2022\)](#) studies the German twin-bond issuance, documenting a greenium based on raw yield differences that widens since 2020. [D'Amico, Klausmann and Pancost \(2023\)](#) leverages this German issuance of green and conventional bonds to estimate a term-structure model to isolate a "benchmark greenium" purged of non-environmental factors. We study a setting without twin bonds, and we are able to measure a greenium with a set of bonds with different maturities by estimating a statistical asset-pricing model. We emphasize the term-structure of green and conventional bonds, showing it is informative about the different risk-properties of green bonds and convenience yields more generally. [D'Amico et al. \(2023\)](#) also find a downward sloping greenium curve, for a different albeit overlapping time period and using German bonds. We propose an asset pricing theory based on preferences for real value of green bonds that can rationalize this term-structure fact. In terms of modelling choices, their setup is tractable, with prices being a linear function of state variables, following the linearity-generating processes assumptions in [Gabaix \(2012\)](#). We estimate an exponentially-affine model, so in our setup prices are log-linear in states ([Duffie and Kan \(1996\)](#) and [Ang and Piazzesi \(2003\)](#)). We also show that no-arbitrage term-structure models are useful beyond the twin bond setting and our measurement strategy shows how sovereigns and investors can evaluate pricing counterfactuals even in the absence of identical securities. [Bretschler, Hsu and Tamoni \(2020\)](#) shows how fiscal policy shock affects bond risk-premia, while our findings suggest that sovereign green issuance can also have an effect on green bond risk-premia. Speaking to the credibility of Chile's green bond program, [Cheng, Jondeau and Mojon \(2022\)](#) shows that Chile would receive the highest weights in a sovereign bond portfolio that aimed to minimize carbon footprint.

On mechanisms, [Giglio, Kelly and Stroebel \(2021\)](#) survey macro-finance models that incorporate climate concerns. Among these are models where agents have non-consequentialist (warm-glow) preferences over green securities. Our theory builds on this class of models. In equilibrium, such preferences create a convenience yield and lower expected returns for green assets ([Pástor, Stambaugh and Taylor \(2021\)](#); [Pedersen, Fitzgibbons and Pomorski \(2021\)](#)). [Chikhani and Renne \(2025\)](#) show that climate risk will increasingly drive down long-term risk-free yields; here we show that even short-term macroeconomic risk has the potential to drive down long-term green bond yields by commanding a green bond specific risk-premium. [Sauzet and Zerbib \(2022\)](#) introduce preference for green goods in a general equilibrium setting, which they show is a limiting force on the impact of green investing, since brown assets become a hedge for green consumption. Our theory is also a risk-based explanation, where green bond also becomes a bad hedge for green preferences. We also connect to recent theory linking asset returns and climate policy: [Chittaro, Piazzesi, Schneider and Sena \(2025\)](#) and [Pedersen \(2025\)](#) show how cross-sectional return wedges can mimic carbon taxes, which in our sovereign-bond context implies that a maturity-varying greenium provides a price-based incentive for sovereign green projects. [Sauzet \(2024\)](#) studies whether green investors can still have an impact in the presence of financial intermediaries, finding that a greenium emerges even when intermediaries are not environmentally minded. Our theory also relates to [Aron-Dine, Beutel, Piazzesi and Schneider \(2024\)](#) who provide a new survey on households portfolio choice for green assets to quantify an asset pricing model with nonpecuniary benefits and hedging demand. While we do not allow for hedging demand, our mechanism obtains with or without it. Our emphasis on the role of risk in determining the greenium term-structure echoes findings in [Hong, Kubik and Shore \(2025\)](#) that finds that green-asset volatility is a key determinant of decarbonization. Here, we show the existence of risk specific for green bonds, which can significantly diminish greenium in long-term bonds.

Our notion of a green convenience yield relates to a broader literature that views certain assets as delivering nonpecuniary services, typically from safety or liquidity services, that lower required returns. This literature dates back to papers studying money convenience ([Sidrauski \(1969\)](#), [Lucas \(2000\)](#)). In the Treasury market, [Krishnamurthy and Vissing-Jorgensen \(2012\)](#) quantify these services, using debt-supply variation to estimate an average convenience yield on the order of tens of basis points. [Nagel \(2016\)](#) show that liquidity premia for near-money assets comove positively with short-term interest rates. In our sample, short-term greenia correlates positively with inflation. More recent work demonstrates that these premia can flip sign when intermediation frictions dominate: during March 2020, dealer balance-sheet constraints generated inconvenience yields with Treasury–OIS spreads turning positive [He, Nagel and Song \(2022\)](#); post global financial crisis, a regime shift in which dealers became net long Treasuries helps rationalize negative swap spreads and their connection to funding stresses

[Du, Hébert and Li \(2023\)](#); and at the front end, T-bill yields have at times exceeded other risk-free benchmarks when dealer balance-sheet constraints bind [Klingler and Sundaresan \(2023\)](#). We also estimate time-varying greenium term-structure, especially at shorter maturities.

Outline. The rest of the paper is organized as follows. In the next section we provide institutional background on Chile's green bond program and outline the data sources. Section 3 presents how we measure pricing differentials and risk exposure by estimating an exponentially affine model for green and conventional bonds. In Section 4 we present facts on liquidity and holdings of Chilean sovereign green bonds, arguing they do not explain price differences between green and conventional bonds. In Section 5 we develop a an asset pricing model with nonpecuniary benefit for real green bond portfolio holding that shows how inflation risk can rationalize the downward sloping greenium term-structure.

2. Data and Setting: The Chile Green Bond Program

This paper estimates a term-structure model and establishes facts about Chilean green bonds. This section gives institutional context on the Chilean green bond program and describes the different datasets from which we draw, indicating their main purpose in the analysis.

2.1. Chile Green Bond Program

Chile's sovereign green bond program began in 2019 as a Ministry of Finance initiative to finance climate-aligned public investment while signaling policy commitment and setting a regional benchmark for sovereign sustainable finance. The government approved its Green Bond Framework in May 2019, defining eligible sectors (clean transportation, energy efficiency, renewable energy, living natural resources and protected areas, water management, and green buildings) and committing to annual allocation and impact reports to ensure transparency for investors. Implementation is overseen by an inter-ministerial Sustainable/Green Bonds Committee led by the Ministry of Finance with support from the Ministry of Environment; the committee screens expenditures, links issuances to certified project portfolios, and coordinates reporting in line with Climate Bonds Initiative and International Capital Market Association (ICMA) guidance. The program's stated policy logic is twofold: mobilize low-cost funding for Chile's transition to a low-carbon, climate-resilient economy and establish a sovereign benchmark to catalyze domestic and regional sustainable debt markets.

Issuance has been frequent and staged across currencies since the debut. We focus on green and sustainable dollar bonds. It is worth emphasizing that sovereigns typically issue green bonds in foreign currency, even in Chile, which traditionally has most of its outstanding debt in local

currency. Until 2022, all bonds issued were of the use-of-proceeds type, where bond issuances are linked to specific projects. In 2022, Chile became the first sovereign to issue sustainability-linked bonds (SLBs). This is a different bond design that allows general budget financing while embedding step-up coupons if predefined key performance indicators (KPIs) are missed. This structure can be preferred by sovereign treasuries because it preserves financing flexibility (no ring-fencing of proceeds), while the contractual incentives to meet economy-wide environmental targets preserve green signalling. Such an issuance could potentially lower funding costs by also targeting investors' with a higher willingness to pay for environmentally-aligned bonds, if investors perceive that issuers have set credible and meaningful targets. As we show in Section 3.5, we find that indeed SLBs are priced as cheaply as use-of-proceeds green bonds.

Chile has explicitly marketed its program around transparency and is subject to third-party verification to address greenwashing concerns. For example, its first issuance was reviewed by Vigeo Eiris, a global leader in ESG assessments. In its report on Chile's debut green bond dollar issuance, the reviewer states to be "of the opinion that the Sustainable Bond Framework of the Republic of Chile is aligned... with core components... and adopts best market practices....". We are not aware of allegations of misallocation in Chile's sovereign green bond program. The annual government reports and external assurance documents reinforce the good reputation of Chile's green bond program. These governance features make it sensible for investors to treat green bonds differently from conventional bonds. As evidence of market confidence, Chile's inaugural issuance was met with overwhelming demand, being oversubscribed by 12.8 times. Other issuances, including SLBs, were also oversubscribed.¹

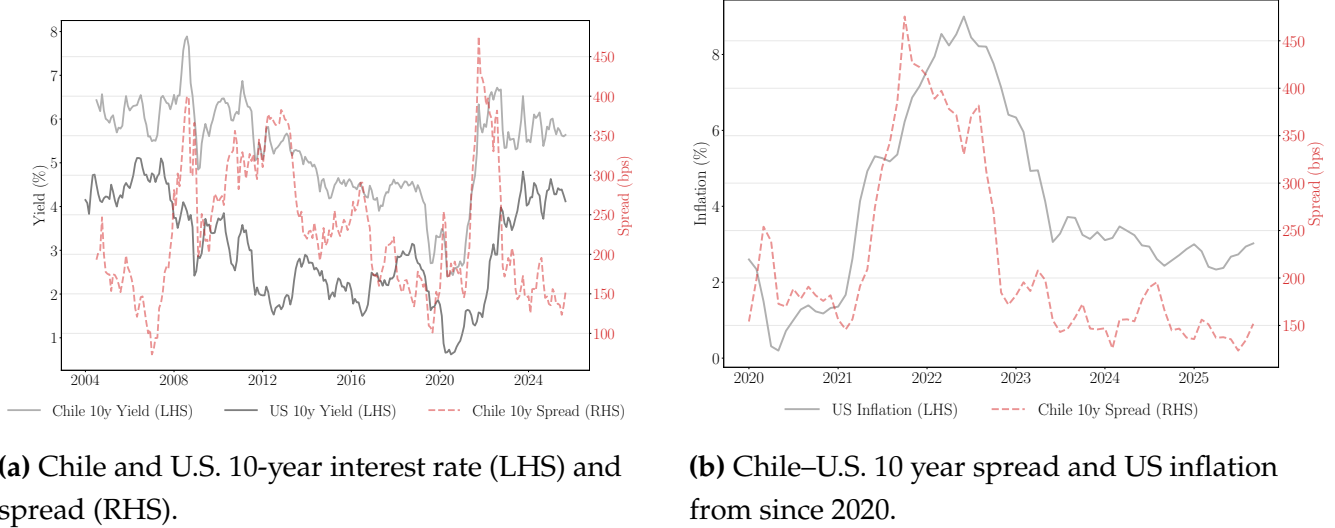
Since 2019, the Chilean government has issued USD 24 Bn in green bonds. With an average greenium of 20 bps, this amounts to about USD 48 million in annual interest-rate savings by issuing a green instead of an otherwise identical conventional bond. This represents around 1% of Chile's annual budget deficit. In terms of size, the total amount of Chilean dollar green bonds represents around one third of the total amount of Chilean dollar bonds and around 10% of the total debt burden of Chile. Over our sample period from 2019-2024, Chile's debt-to-GDP was around 40%.

Relative to peers, Chile has been an early mover: it was the first sovereign in the Americas to issue a green bond, as well as the first sovereign in the world to issue an SLB in 2022. For SLB's it was followed by Uruguay, and more recently Thailand (2024) and Slovenia (2025), with other sovereigns such as Brazil signaling interest in such an issuance. Our findings here on the Chilean program can therefore provide useful lessons for other sovereigns that aim to establish a credible green bond framework.

Finally, Chile is a relatively fiscally sound country. It has a high credit rating among emerging

¹<https://old.hacienda.cl/oficina-de-la-deuda-publica/bonos-verdes/notas-de-prensa-sobre-bonos-verdes/chile-obtiene-tasa-historicamente-baja-652676.html?>

markets borrowers (ratings are investment grade, with Moody's A2, S&P A, Fitch A- during 2024-25), with among the lowest CDS spreads in emerging markets. As a result, dollar yields on Chilean bonds move largely with U.S. Treasuries rather than idiosyncratic default risk. Figure 1 illustrates this. Panel 1a shows the co-movement of Chile and U.S. 10-year interest rates and Panel 1b shows the co-movement of the 10-year spread and US inflation since 2020. The main driver of recent movements in the spread was post-pandemic inflation, and not credit spreads widening because of higher idiosyncratic default risk. This motivates our choice of inflation as a risk factor in our quantitative asset pricing model in Section 5.



(a) Chile and U.S. 10-year interest rate (LHS) and spread (RHS).

(b) Chile–U.S. 10 year spread and US inflation from since 2020.

Figure 1: Chile and U.S. 10 year interest rates and US inflation.

2.2. Data Sources

We draw from three different data sources: Bloomberg for prices, eMAXX for bond holdings and Luxembourg Stock Exchange for green bond contractual details.

2.2.1. Prices

We obtain all prices and yields from the Bloomberg Terminal, as well as other relevant financial information, such as bid-ask spreads and pricing sources. In Appendix A.1 we present detailed information on each bond used in our estimation.

2.2.2. Holdings Data

We use the eMAXX database from Thomson Reuters. It is a proprietary dataset that provides comprehensive, quarterly, security-level data on the holdings of fixed income securities by

institutional investors, including insurance companies, mutual funds, and pension funds. The funds are primarily based in the United States. Holdings are aggregated from regulatory disclosures by asset managers and institutional investors. eMAXX does not cover households, banks, or governments. Sample selection is based on availability of regulatory disclosure, e.g., insurance companies' reports to the National Association of Insurance Commissioners and mutual funds' U.S. Securities and Exchange Commission (SEC) filings. The data also contain characteristics of individual bonds and firms. We use this data to track a panel of funds that hold both the green and non-green Chilean bonds.

2.2.3. Green Bonds Data

We source green bond data from Luxembourg Stock Exchange (LuxSE), a leading venue for the listing of green bonds, hosting a wide variety of sustainable debt instruments on its exchange. The selection and classification of green bonds follow internationally recognized standards and strict eligibility criteria to ensure integrity and transparency. The data is available through the LuxSE data platform, which provides detailed information on green bond issuances, including issuance date, maturity, coupon, and other contractual characteristics, such as the eligible expenditures for use of proceeds bonds and the conditions for step-up coupon payments for the sustainability-linked bonds. For our purposes, we use only Chilean green, sustainability and sustainability-linked dollar bonds.

3. Affine Term-Structure Model for Green Bonds

Investors are willing to pay more for short- and medium-dated green exposure but not for very long maturities, which manifests as a steeper green yield curve that converges to the non-green curve at long horizons. A two-factor, no-arbitrage term-structure model with separate pricing kernels for green and non-green bonds uncovers a 20 bps greenium for short maturities that declines toward zero at the long end. This is driven by both different short-rate and different market prices for interest-rate risk.

3.1. Asset-Pricing Model

Setup. We price coupon Chilean sovereign bonds with two estimated SDFs, indexed by $j \in \{G, C\}$ for green and conventional bonds. The SDFs share state dynamics, but differ in short rate and market prices of risk. We adopt the exponentially affine specification ([Duffie and Kan \(1996\)](#), [Ang and Piazzesi \(2003\)](#)), a parsimonious and tractable specification that clarifies the different pricing properties of both sets of bonds.

For an n -period cash-flow claim,

$$P_t^{(n),j} = \mathbb{E}_t \left[M_{t+1}^j P_{t+1}^{(n-1),j} \right], \quad M_{t+1}^j = \exp \left(-r_t^j - \frac{1}{2} \Lambda_t^{j'} \Lambda_t^j + \Lambda_t^{j'} \varepsilon_{t+1} \right), \quad (1)$$

where the state shocks satisfy $\varepsilon_{t+1} \sim \mathcal{N}(0, I)$.

The market prices of risk and short-rate are affine in the state,

$$\Lambda_t^j = \Lambda_0^j + \Lambda_1^j z_t \quad (2)$$

$$r_t^j = \rho_0^j + \rho_1^j z_t \quad (3)$$

where ρ_0^j, ρ_1^j govern the short-rate and Λ_0^j, Λ_1^j the market-prices of risk. The state follows a stationary mean zero VAR(1) process,

$$z_t = \Psi z_{t-1} + \Sigma \varepsilon_t \quad (4)$$

The estimated parameters are $\theta_j = (\rho_0^j, \rho_1^j, \Lambda_0^j, \Lambda_1^j, \Psi, \Sigma)$. We first estimate the VAR(1) parameters (Ψ, Σ) and once fixing those, we estimate the SDF parameters $(\rho_0^j, \rho_1^j, \Lambda_0^j, \Lambda_1^j)$ by minimizing the pricing errors for green and conventional bonds.

Factors. For our baseline specification, we use a two dimensional state z_t

$$z_t = (\text{Level}_t, \text{GreenSpread}_t)'$$

where Level_t summarizes the level of the conventional bond term-structure and GreenSpread_t captures systematic differences between green and non-green yields. We use the first principal component of conventional bond yields as the level factor. The level factor explains more than 99% of the cross-sectional and time series variation in non-green bonds. The green spread factor is the difference between the longest maturity conventional and green bond yields. The time period considered in our sample features the sharp interest rate increase following the inflationary shock after COVID-19, which explains how the level factor explains an unusually large share of the variation in yields.

We show in Appendix B a family of alternative specifications that yield similar results. We choose this as our baseline estimate since it shows a good fit of both green and conventional yields with a parsimonious number of factors. Alternative specifications show similar results, as Table 12 in Appendix B shows. The key fact on the greenium term-structure is robust and adding more factors does not improve the fit of the model. Figure 2 shows the time series of factors.

Under (1)-(4), bond prices and yields are exponential-affine in z_t . This structure allows us to trace the greenium directly to differences in short-rate and priced risk, holding the economic environment z_t fixed.

Parameter interpretation. The parameters (ρ_0^j, ρ_1^j) govern the average and the time-varying nature of short-rates, respectively. When investors are risk-neutral, differences between the

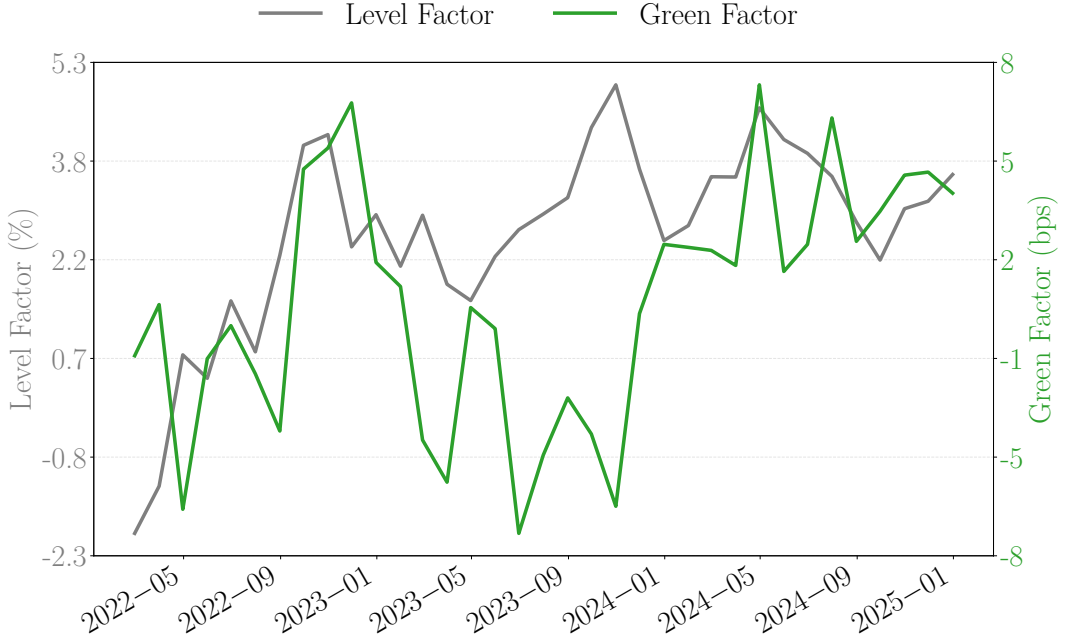


Figure 2: Time series of the level and green spread factors.

pricing of green and conventional bonds would only reflect differences in the expected path of their short-rates. When investors are not risk-neutral, market prices of risk Λ_t^j are also important determinants of bond yields since they determine how the risk-premia react to shocks to the economic state ε_{t+1} . For example, suppose there is one state variable, the level of interest rates. If Λ_t^G is larger than Λ_t^C , then expected excess returns on the green bond are higher than on a conventional bond. In other words, green bonds carry a higher risk-premium. As we show below, this is exactly what we find. Our parameter estimates inform us that high interest rate states of the world are relatively worse for green bonds.

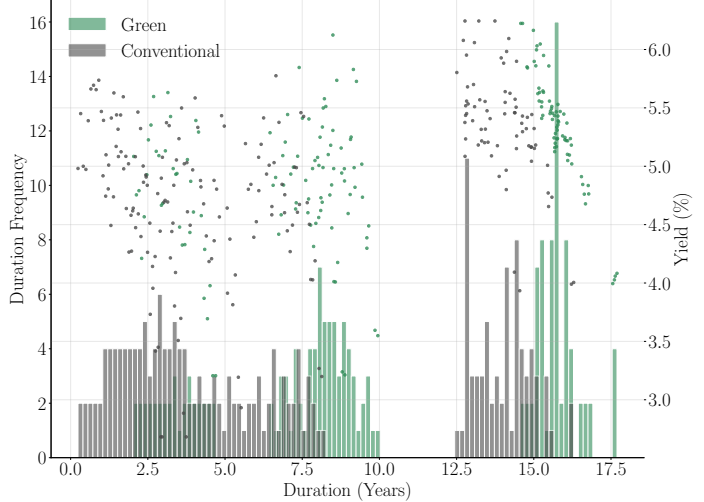
3.2. Estimation and Fit

Method. We estimate the model by pricing the cash flows from every coupon bond and minimizing the squared fitting errors made by the model. In Figure 4 we report the distribution of pricing errors, pooling across bond and time-period. We highlight the different distribution of pricing errors for green and conventional bonds, showing that both are similar in magnitude and distribution. In Appendix B we show the time series fit for green and conventional bonds. Our sample consists of 5 green bonds and 6 conventional dollar denominated Chilean sovereign bonds, from 2019 to 2024. The model is estimated at the monthly frequency, and prices are aggregated from daily data as end of month prices. In Figure 3 we summarize information in our sample of bonds. Panel 3a provides summary statistics and Panel 3b plots the distribution of

duration and yields over our sample period, for green and conventional bonds.

	Green	Non-green
Number of bonds	5	6
Shortest maturity	Jan 2027	Mar 2025
Longest maturity	Jan 2050	Jun 2047
Average issue size (USD bn)	1.8	1.5

(a) Summary statistics for bonds in the estimation sample.



(b) Yield (%) vs duration (years). Each point is a bond–date pair.

Figure 3: Sample coverage across instruments and time.

Regularity Conditions Dynamic exponentially-affine term-structure models commonly face identification and estimation challenges ([Collin-Dufresne et al. \(2008\)](#), [Bauer et al. \(2012\)](#), [Hamilton and Wu \(2012\)](#)). Our choice of using observable factors allow the factor dynamics and the market prices of risk parameters to be estimated separately, which makes the estimation procedure more tractable ([Joslin, Singleton and Zhu \(2011\)](#)). Apart from requiring pricing errors to be minimized, we also impose the following constraints in our estimation that help ensure convergence of the estimator as well as obtaining an estimated SDF that is economically plausible.

In the spirit of [Cochrane and Saa-Requejo \(2000\)](#) and [Jiang, Lustig, Van Nieuwerburgh and Xiaolan \(2024\)](#), we impose “good deal bounds” on our SDF, requiring that the SDFs standard deviation is below 2. We also penalize short-rate estimates that lead to green short-rate that differs by more than 1 percentage point from the non-green short-rate. This can be viewed as an empirically plausible regularization of short-rate parameters, taking heed of prior literature estimates for the literature. Since we do not observe short maturity green bonds, these restrictions are required to discipline the short-end of the green yield term-structure. We do not impose any restriction on the sign of the short greenium. To achieve this, we restrict the short-rate parameters to only allow to differ by a constant and vary with the green spread factor. Further, since most of the SDF variation is driven by the level factor, we restrict that only the price of risk parameter relative to the level factor to vary over time, driven by the level factor itself.

Our baseline estimate has eight parameters, achieving the smallest average fitting error

between green and conventional bonds. Due to our small sample, we restrict the time variation of market prices of risk to be driven only by the level factor. Reducing the number of parameters to estimate allows for more powerful inference, as well as making optimization more tractable. The key fact from our estimated model is borne out of time-invariant part of market prices of risk.

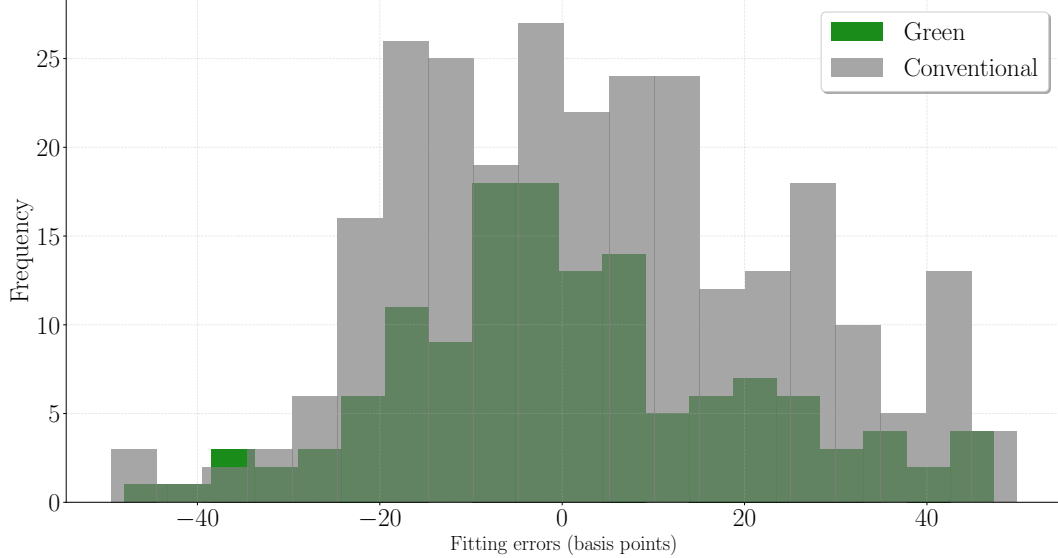


Figure 4: Distribution of pricing errors pooled across bonds and time. Errors are expressed in basis points subtracting observed yields from model implied yields (model minus market price).

Table 1: Average absolute pricing errors by bond type. Errors are expressed in basis points.

(a) Pricing errors for each green bond.

ISIN	Maturity	Error (bps)
US168863DX33	Jan-27	16
US168863DN50	Jan-32	22
US168863DV76	Jan-34	14
US168863DL94	Jan-50	11
US168863DW59	Jan-52	12

(b) Pricing errors for each conventional bond.

ISIN	Maturity	Error (bps)
US168863BW77	Mar-25	16
US168863CA49	Jan-26	15
US168863CF36	Feb-28	21
US168863DP09	Jan-31	18
US168863BP27	Oct-42	17
US168863CE60	Jun-47	15

3.3. Results: Shape and Magnitude of the Greenium

Yield curves. In Figure 5 we plot the model-implied average term-structures (over the time series) for green and conventional bonds. We see that the green curve lies below the conventional

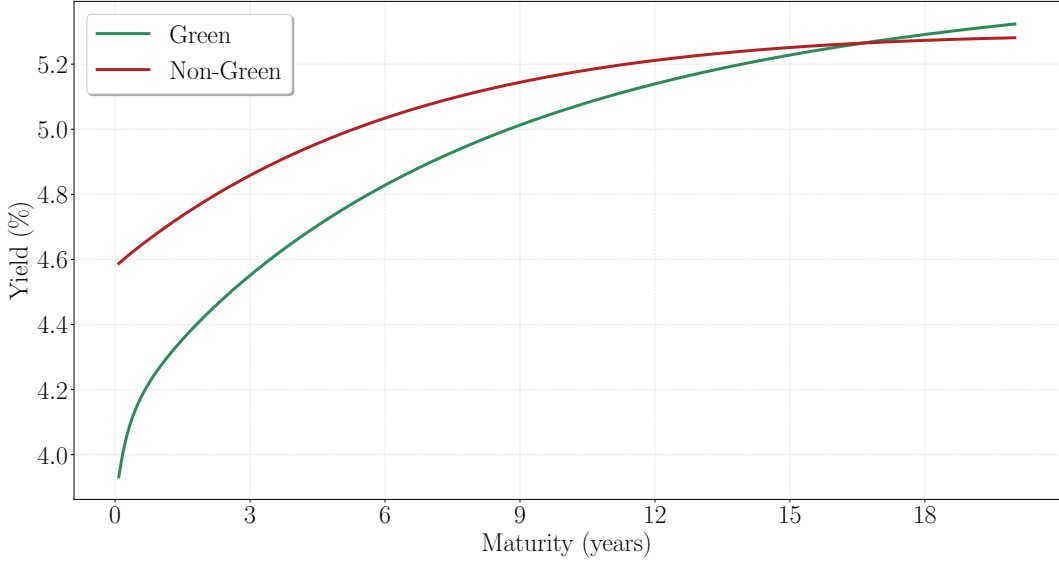


Figure 5: Model-implied average term-structures (over the time series) for green and conventional bonds.

sovereign bond curve. This means that while green bonds are cheaper for the issuer, the expected excess returns are higher for green bonds. Here it is important that the excess return is based on the green short rate rather than the conventional short rate. Since the price of the green bond is higher (its rate is lower) and the payoff at maturity is the same, the expected return on the green bond is lower. However, subtracting a much lower green short rate from that return leads to an expected excess return on green bonds that is higher. Eventually, at around the 20 year maturity, both bonds are priced equally. Figure 6 shows the implied greenium term-structure with 95% confidence intervals obtained from 1000 bootstrap samples, following the method described in [Hamilton and Wu \(2012\)](#).

Table 12 in Appendix B shows that across different specifications, the greenium can vary from 5 bps to around 70bps. While there are short-term coupon bonds in our dataset, their weight in the overall price of bonds is small, so the model largely relies on extrapolation from the shortest-term green bond to infer short-term greenium. Still, the short-term greenium is estimated to be positive across all specifications. As we show below, the key driving forces for our term-structure estimate are the large increase in interest rates in the sample and the concomitant decline in the short-maturity greenium during the same time period.

3.4. What Drives the Results? Different Green Bond Risk Exposure

To gauge drivers of the greenium term-structure, it is useful to inspect the model-implied risk exposure of green and conventional yields. A useful feature of exponentially-affine models is that in spite of the nonlinearity of pricing equations, they lead to an affine relationship between

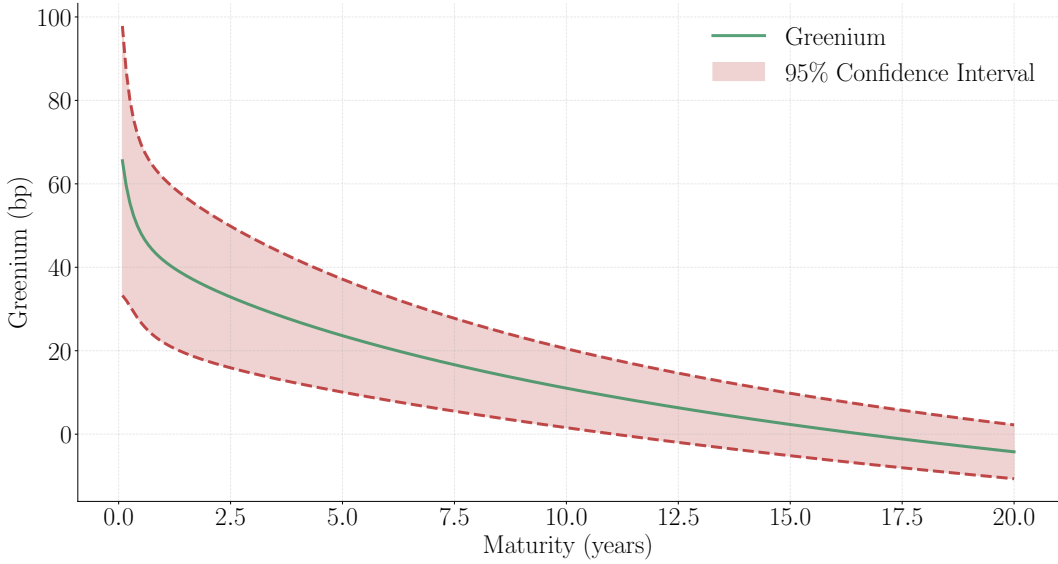


Figure 6: Implied greenium term-structure with 95% confidence intervals obtained from 1000 bootstrap samples.

yields and risk factors, in this case,

$$y_t^{(n),j} = a_j(n) + b_{1,j}(n)\text{Level}_t + b_{2,j}(n)\text{GreenSpread}_t, \quad j \in \{\text{Green, Conventional}\} \quad (5)$$

where the coefficients $a_j(n), b_{1,j}(n), b_{2,j}(n)$ are non-linear transformations of the underlying estimated parameters, that we specify in Appendix B. The parameters $b_{i,j}(n)$ measure the risk-exposure of bond type j to the i -th factor, that is, how much yields change when, for example, the level factor increases. The parameter $a_j(n)$ is the average yield at maturity n . In Figure 7 we plot these estimated parameters for green and conventional bonds. We see that the constant coefficients mimic the estimated term-structure shape, which means that on average the greenium term-structure is downward sloping. Further, we see that green bonds are more exposed to interest rate risk, here represented by the level factor. When interest rates increase, yields on green bonds increase by more than conventional bonds, especially at the short end. This means that as interest rates increase, which is the case in our sample, the greenium term-structure flattens.

Evidence from matched bonds. In order to inspect the raw features in the data that lead to these estimates, we construct approximate greenium by matching green and conventional bonds of similar maturity. By taking the difference in yields between pairs, we have the conventional greenium measure in the literature, albeit here it noisily measured due to maturity mismatch. The plot shows that short-term greenium decreases when interest rates rise, while long-term greenium hovers around zero, in line with the estimated exposures in Figure 7.

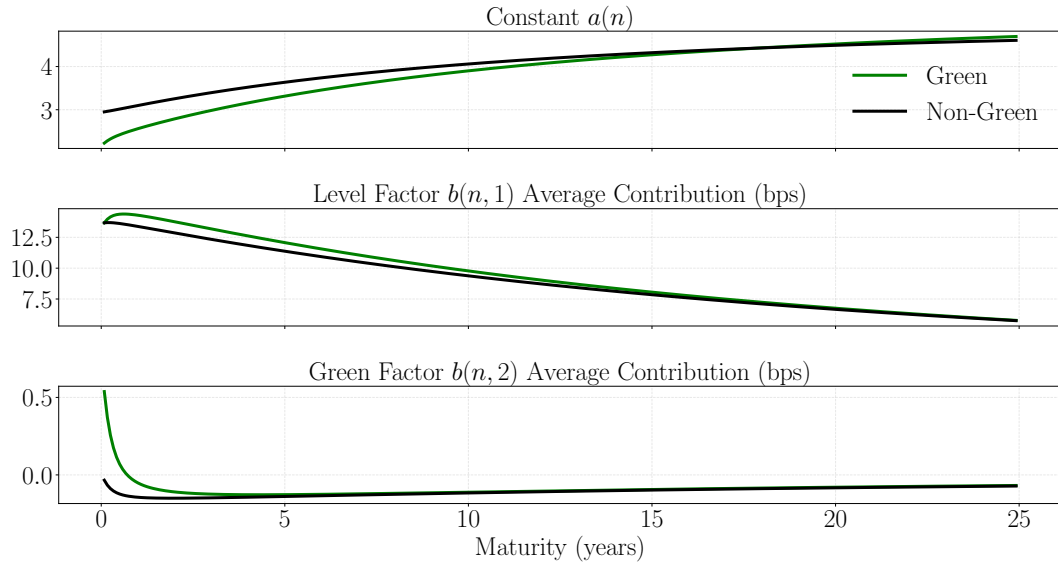


Figure 7: Estimated risk-exposure of green and conventional bonds to the level and green spread factors.



Figure 8: Approximate greenium term-structure constructed by matching green and conventional bonds of similar maturity. We use as a measure of short-rate an index of short-term interest rates for corporates rated A, which is the same credit rating as Chile.

A direct implication is that the greenium term-structure should flatten over our sample. This is indeed recovered from our SDF estimates, as shown in Figure 9.

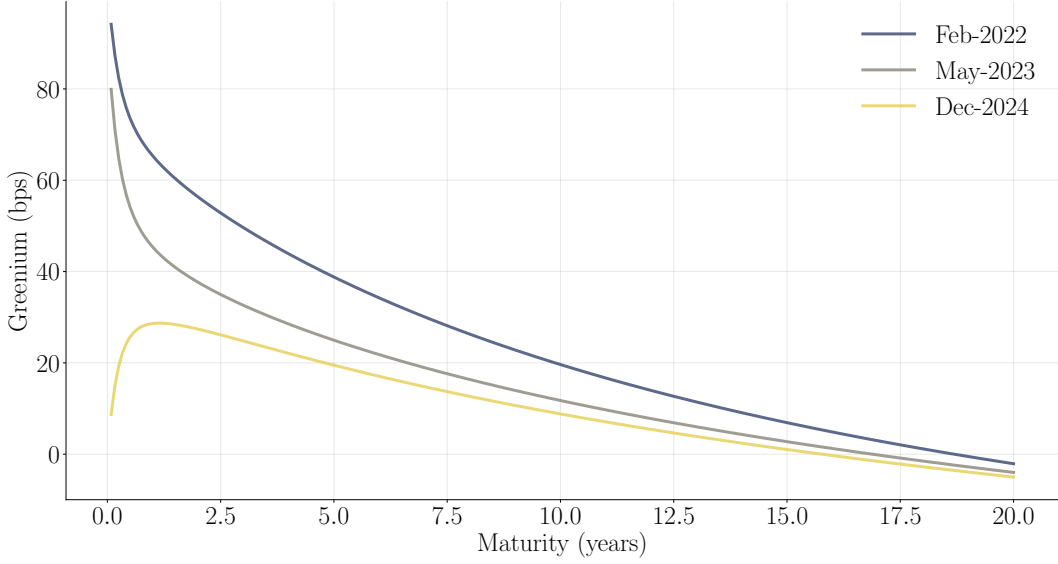


Figure 9: Greenium term-structure over 3 dates in our sample period.

The role of priced risk. Finally, to understand the role of priced risk versus expected short-rate path, we plot the greenium term-structure implied by the model if we assume that green bonds are priced with the same market prices of risk as conventional bonds. We set the green market prices of risk to be the same as the conventional market prices of risk.

$$\Lambda_0^G = \Lambda_0^C, \Lambda_1^G = \Lambda_1^C \quad (6)$$

Figure 10 shows that the result of this exercise, showing we get a mostly flat greenium term-structure. This echoes the findings in the previous section in that exposure to risk factors is what mostly drives the estimated downward slope of the greenium term-structure.

3.5. Do SLB's provide cheaper financing and meaningful financial incentives?

The SLB bond design is an attempt to align issuers environmental incentives by requiring bond coupon payments to be contingent on environmental targets, but differently from a standard green bond it does not tie the proceeds to specific projects. Chile is a pioneer in this area, having issued the first sovereign SLB in 2022. Can such an instrument reduce a sovereign's borrowing cost? Do current Chile's SLBs provide cheap financing like use-of-proceeds bonds? How big are the financial incentives in the state contingent coupon payments? In this section we use our estimated SDF to inform these questions. We show that SLBs are indeed priced as cheaply as

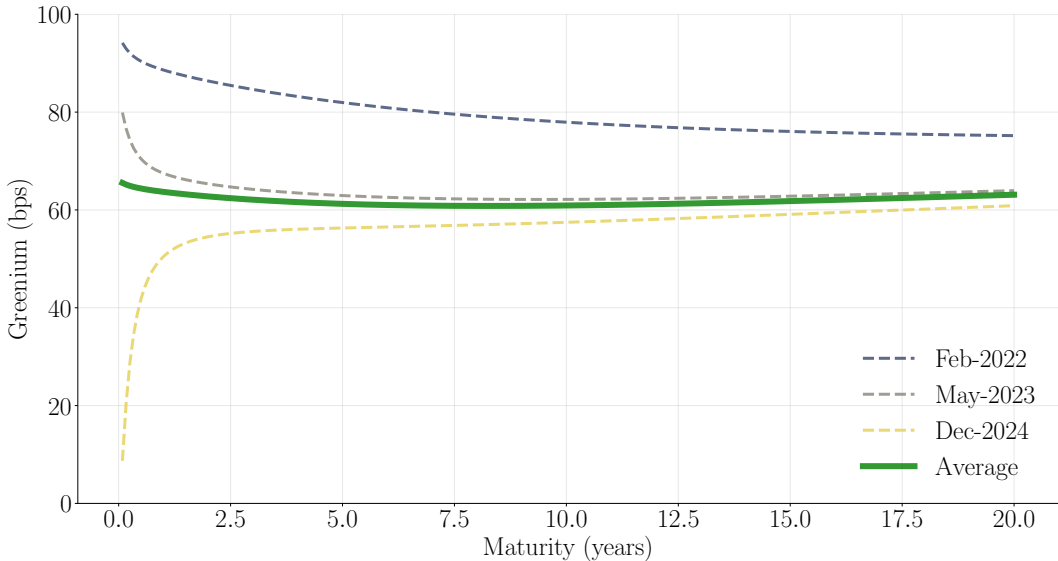


Figure 10: Greenium term-structure implied by the model if we assume that green bonds are priced with the same market prices of risk as conventional bonds. Thick green line is the time-series average of the term-structure and colored lines plot the term-structure at the specified dates.

regular use-of-proceeds bonds, especially at short maturities, echoing our term-structure finding. This is in spite of the current coupon penalties being relatively small, as we also show. These findings suggest that Chile's signalling of environmental commitment being the main driver of the greenium, not the type of instrument.

3.5.1. Are SLBs priced like regular green bonds?

Yes. To reach this conclusion, we use our estimated SDF's to price SLBs cash-flows and compare them with market prices. Figure 11 shows the example for the 2036 SLB. We see that the green pricing kernel prices closely to market prices, whereas the conventional SDF prices consistently lower.

We repeat this exercise for the two other SLB bonds. Since these are longer maturities, we find no material price difference when pricing with either the green or conventional SDF. This should not be surprising given that we find that discount rates for both SDFs converge for long maturities. This therefore echoes the previous finding; SLBs are cheaper here when issued at short maturities. For the SLB design, this also means that setting short-maturity step ups also provide relatively larger financial incentives.

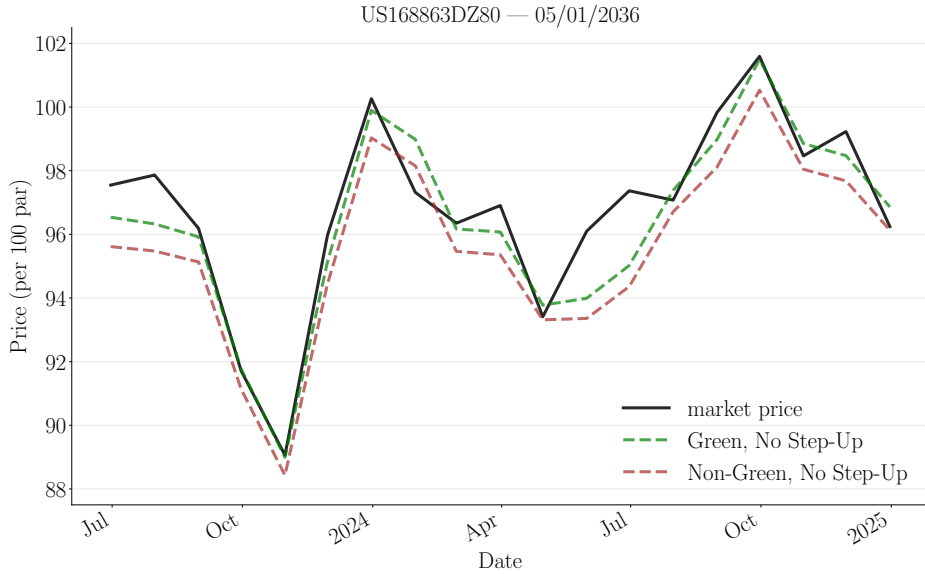


Figure 11: Time-series of SLB prices implied by the green and conventional SDFs.

3.5.2. How large are SLB coupon incentives?

Between 2 and 10bps in annual financing costs. To reach this conclusion, we use the estimated SDF to price SLBs cash-flows under each step-up scenario. We then translate price differences from each step-up scenario to the yield equivalent change, what we define as a yield subsidy. This is a subsidy since the step-up option makes the SLB more expensive, and so reduces the issuer's financing cost by providing this option.

To calculate this yield subsidy, we compute the yield change under the baseline cash-flows (no step-up) that leads to the same price obtained when coupons step-up. This quantity is the answer to the following question: the step-up option value is a subsidy to the issuer since it makes the bond more expensive today; what is this subsidy expressed in yield-equivalent terms? Put differently, it gives the financial penalty if the bond indeed steps up in terms of annual financing costs.

Table 2 below summarizes this quantity for the three sovereign dollar SLB bonds issued by Chile. The main takeaway is that discounting significantly reduces the financial incentives in the SLB state-contingent coupon payments. This means that the embedded financial incentives in coupon step-ups has room to be larger. It also suggests that risk in coupon payments are currently small, which can be useful for sovereign issuance if environmental signalling is the main objective with SLB issuance.

ISIN	Step-up scenario (bps)	Maturity	Step-up yield equivalent (bps)
US168863DY16	12	July-2042	4
US168863DY16	25	July-2042	9
US168863DZ80	25	May-2036	4
US168863DZ80	50	May-2036	8
US168863EA21	5	May-2054	2
US168863EA21	10	May-2054	5

Table 2: SLB Step-Up Yield Subsidy (in bps). We define the yield subsidy as the yield required to match the bond price with cash-flows under the step-up scenario, but with the baseline bond cash-flows.

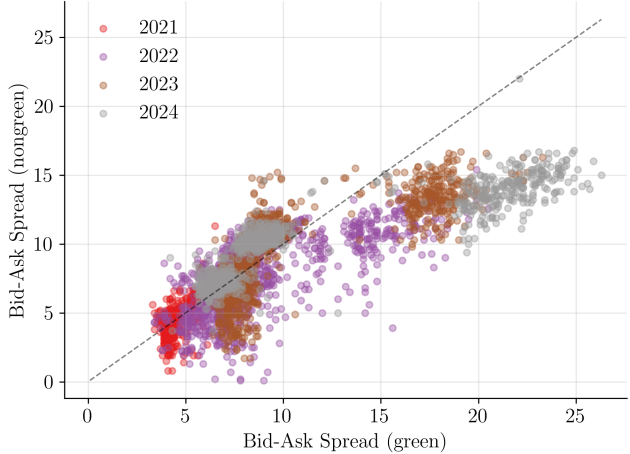
4. Facts on Green Bond Liquidity and Holders

We state two facts related to liquidity and holdings of green and conventional bonds. These facts motivate the representative-agent model with preference for real green bond portfolio.

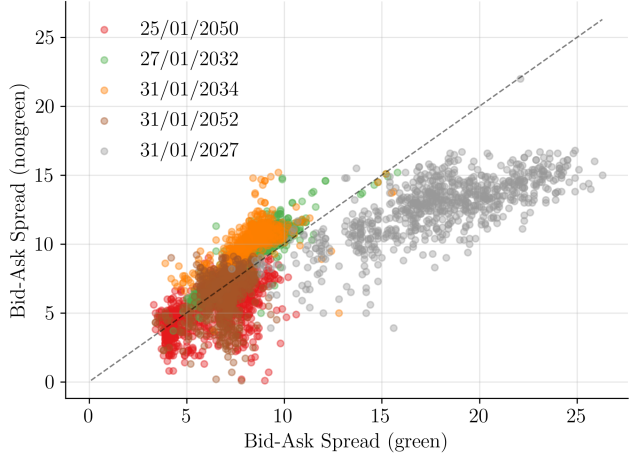
Liquidity on green and non-green bonds is similar Green and conventional bonds exhibit similar liquidity. We show this in Figure 12, by plotting the scatter of bid-ask spreads for matched green and conventional bonds.

The plot shows that bid-ask spreads are of around 15bps and line up close to the 45-degree line across maturities and years. We interpret this as evidence that liquidity of green and conventional bonds of similar maturities are similar. Panel 12a color codes by observation year, while Panel 12b color codes by maturity of the green bond in the pair. We see bid-ask spread variation both over time and across bond maturity, where the most significant illiquidity arises for the short-term green bonds, especially in 2024. While the difference is not big, of around 5-10bps extra bid-ask spread for the green bond pair, the presence of liquidity premia in green yields would lead us to underestimate the greenium for short-maturity. Since we find relatively larger greenia, this leads us to conclude that liquidity cannot solely explain the magnitudes we find. For the main fact of this paper, of a downward sloping greenium term-structure, this is even more true since bonds of longer maturities are more alike.

In summary, because bid-ask spreads are a standard proxy for trading frictions, this evidence implies that liquidity is unlikely to be the channel behind observed price differences between green and conventional bonds.



(a) Panel A: By year



(b) Panel B: By bond maturity

Figure 12: Bid-ask spreads for green and non-green bonds by year (left) and by bond maturity (right).

Common investor base The investor base for green and conventional bonds is largely the same. To show this fact, we plot in Figure 13 the share of funds that hold both green and conventional bonds in the same quarter, the time frequency of our holdings data. This share is computed over the sample of funds in our sample that hold at least one Chilean bond. The plot shows that in the beginning of the sample this share is high and increases, likely due to further issuance of new green bonds. At the end, around two-thirds of the funds hold both a green and a conventional Chilean sovereign dollar bond. This overlap rules out clientele segmentation in which for example green funds would be the primary holder of green bonds but not of the conventional bonds. Instead, we interpret our results as evidence that the same managers evaluate and price both green and conventional bonds, so differences in outcomes should be interpreted as within-investor assessments rather than cross-investor demand shifts. This interpretation guides our modelling assumption for the greenium based on investor preferences.

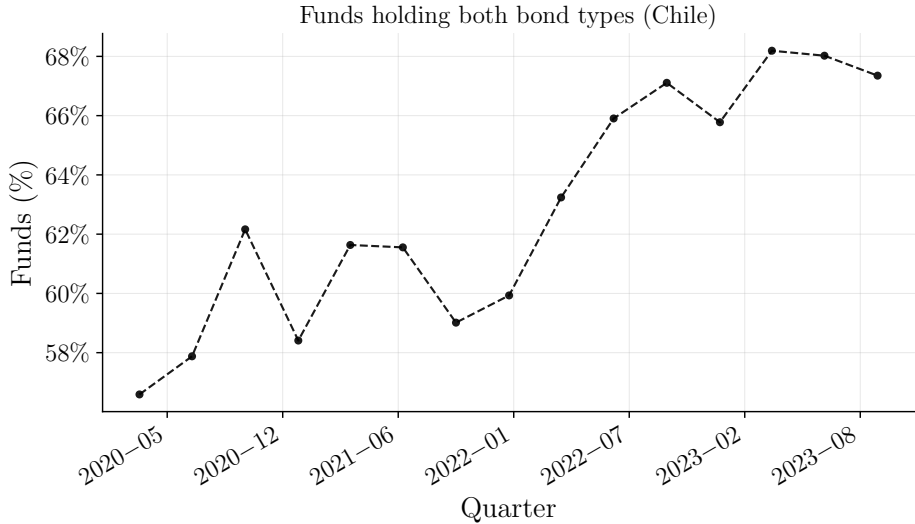


Figure 13: Share of funds that simultaneously hold at least one Chilean sovereign green bond and one conventional (non-green) bond in the same quarter. Sample restricted to funds that hold at least one Chilean bond.

5. Rationalizing the Greenium Term-Structure

The previous section has documented new facts on the pricing of green bonds at different maturities. This section develops an asset pricing model for the term-structure of green bonds in the presence of nonpecuniary benefits for real green bond portfolio. Because inflation is a salient source of risk in our sample, the model emphasizes how inflation shocks move both discount rates and the convenience yield. However the argument that risk in convenience yields is an important determinant in the greenium, especially at longer maturities, extends to other environments and sources of convenience yields.

5.1. Environment

A representative agent has preferences over consumption and green portfolio value

$$E_0 \sum_{t=0}^{\infty} \beta^t u(C_t, G_t) \quad (7)$$

There are $2N$ bonds traded, where N bonds are green and N are conventional. For each type, bonds with maturities $n \in \{1, \dots, N\}$ are traded. We take one time period to be a year. The real

green bond portfolio G_t is defined as

$$G_t := \frac{\sum_{n=1}^N Q_t^{g,(n-1)} B_{t-1,g}^{(n)}}{P_t} \quad (8)$$

where P_t is the price level, $B_{t-1,g}^{(n-1)}$ are the number of bonds of maturity n bought at time $t-1$ and $Q_t^{g,(n-1)}$ is the nominal bond price of the green bond with maturity $n-1$ at time t .

The agent's budget constraint is

$$P_t C_t + \sum_{n=1}^N Q_{t,g}^{(n)} B_{t,g}^{(n)} + \sum_{n=1}^N Q_t^{(n)} B_t^{(n)} = \sum_{n=1}^N Q_{t,g}^{(n-1)} B_{t-1,g}^{(n)} + \sum_{n=1}^N Q_t^{(n-1)} B_{t-1}^{(n)} + P_t I_t \quad (9)$$

where bonds are nominal and upon maturity it pays $Q_t^{(0)} = P_{t-1}$. I_t is an exogenous source of income. We assume inflation π_{t+1} is a persistent process:

$$\pi_{t+1} := \ln \frac{P_{t+1}}{P_t} = \pi_0 + \rho_\pi \pi_t + \sigma_\pi \varepsilon_{t+1,\pi} \quad (10)$$

The novel feature here is inflation as a risk factor for green convenience. This convenience yield is determined by the marginal rate of substitution between the green bond portfolio and consumption.

$$Q_t^{g,(n)} = E_t \left[M_{t+1} (1 + Y_{t+1}) Q_{t+1}^{g,(n-1)} \right], \quad Y_{t+1} := \frac{u_{G,t+1}}{u_{C,t+1}} \quad (11)$$

$$M_{t+1} = \beta \frac{u_{1,t+1}}{u_{1,t}} \exp(-\pi_{t+1}) \quad (12)$$

$$M_{t+1}^g := M_{t+1} (1 + Y_{t+1}) \quad (13)$$

where M_{t+1} is the nominal pricing kernel. We define the product $M_{t+1} (1 + Y_{t+1})$ as the green pricing kernel M_{t+1}^g . Differences in the estimated SDF using green and conventional bonds, as we do in our empirical SDF estimation, recover the stochastic properties of the convenience term $1 + Y_{t+1}$.

Greenium term-structure decomposition Below we state general conditions on the stochastic processes for the SDF and green convenience yields that shape the greenium term-structure. This clarifies how the equilibrium dynamics in our model explains the downward slope of the greenium term-structure. We assume

Assumption 1 (Log-normality and homoskedastic second moments).

- (a) For each $j \geq 1$, (m_{t+j}, y_{t+j}) is conditionally Gaussian given the information set at time t .
- (b) Conditional second moments are homoskedastic.

The greenium term-structure can be decomposed by

Proposition 1 (greenium term-structure decomposition). *For every integer $h \geq 1$,*

$$h g_t^{(h)} := h \left(\log Q_{t,g}^{(h)} - \log Q_t^{(h)} \right) = \sum_{j=1}^h \mathbb{E}_t [y_{t+j}] + \frac{1}{2} \text{Var}_t \left(\sum_{j=1}^h y_{t+j} \right) + \text{Cov}_t \left(\sum_{j=1}^h m_{t+j}, \sum_{j=1}^h y_{t+j} \right). \quad (14)$$

The proof is in Appendix C. The presence of stochastic convenience yields introduce standard asset pricing covariance terms between the stochastic discount factor and the convenience yield. In analogy to theories of the term-structure, the greenium term-structure is determined by the expected path for the short-greenium $\{E_t[y_{t+j}]\}_j$ and convenience risk $\text{Cov}_t \left(\sum_{j=1}^h m_{t+j}, \sum_{j=1}^h y_{t+j} \right)$. We note also the presence of a Jensen term $\frac{1}{2} \text{Var}_t \left(\sum_{j=1}^h y_{t+j} \right)$ in the expected greenium, but which is typically quantitatively small. Relative to the risk-neutral greenium expectations path, the greenium term-structure will slope upward whenever the conditional covariance between the marginal green asset benefit and the stochastic discount factor is positive, and downward sloping when the covariance is negative.

5.2. Quantifying inflation risk in green convenience

The model explains qualitatively the downward slope of the greenium term-structure based on inflation as the macroeconomic risk-factor. We show this in a parsimonious asset pricing model whose only risk-factor is inflation. Quantitatively, it can explain around 15% of the slope of the greenium term-structure.

Calibration We calibrate the asset pricing model with CES preferences over consumption and green bond portfolio.

$$u(C_t, G_t) = \frac{1}{1-\gamma} \left(\left(C_t^{\frac{\eta-1}{\eta}} + \omega G_t^{\frac{\eta-1}{\eta}} \right)^{\frac{\eta}{\eta-1}} \right)^{1-\gamma}. \quad (15)$$

This leads to the following structural convenience function:

$$Y_{t+1} = \omega \left(\frac{C_{t+1}}{G_{t+1}} \right)^{\frac{1}{\eta}}. \quad (16)$$

To isolate the role of inflation risk, we let consumption be deterministic, $C_t \equiv \mu_c$, and take inflation as the sole shock. We calibrate the model to match the short-term rate and volatility of the data, as well as the level of the short-term greenium.

Table 3: Model Calibration Parameters

Parameter	Description	Value	Source
<i>internally calibrated parameters</i>			
β	Discount factor	0.99	-
ω	Green bond portfolio preference weight	0.09	-
μ_c	mean consumption	1.02	-
<i>externally calibrated parameters</i>			
μ_π	Mean inflation	0.02	US inflation target
ρ_π	Persistence of inflation	0.97	estimated
σ_x	Std. dev. of inflation expectations shock (%)	0.50	estimated
γ	Risk aversion	5.00	Hall (1988)
η	intratemporal preference elasticity of substitution	1.00	Cobb-Douglas preferences

Table 4: Model Calibration Parameters. Internally calibrated parameters are set to match the mean of the short-rate, the mean short-greenium and the greenium slope. Externally calibrated parameters are set externally to any moment matching, with values either taken from the literature, estimated on time-series data or set to impose parametric restrictions on functional forms.

We simulate the model at a yearly frequency and compute the unconditional moments of interest rates and greenium. Table 5 summarizes the main moments in the data and model.

Moment	Data	Model
Mean short rate (annual, %)	4.59	4.84
Mean short greenium (bps)	59.66	57.30
Greenium slope (bps/year)	-1.39	-0.21
Correlation Convenience and SDF	-0.442	-0.744
Correlation Inflation and Greenium Slope	-0.588	-0.992

Table 5: Moments: Data vs Model

Mechanism for a downward sloping greenium term-structure In this environment states of high inflation states are states of low real green bond portfolio value. Our assumption on preferences implies a decreasing marginal convenience, so these are states of scarce and thus more valuable convenience. This leads to a negative covariance between the nominal stochastic discount factor and convenience yields, since here high inflation states are good states of the

world, with low values for the nominal SDF, as per (12). Here we emphasize inflation as a risk-factor for green convenience, since it was a salient source of risk in our sample. Quantitatively, inflation risk alone can drive up to 20% of the decrease in the greenium at longer maturities.

Consistent with the theoretical greenium term-structure decomposition (65), the model predicts a negative covariance between the stochastic discount factor and convenience yields as well as a negative correlation between inflation and the slope of the greenium. This is consistent with our empirical evidence: we find indeed that the slope of the greenium term-structure flattens when inflation reduces, as per Figure 8.

6. Conclusion

Green borrowing can be materially cheaper at short maturities, but carry a different risk exposure. These are useful for sovereigns when planning green bond issuance and for investors when choosing between green and conventional bonds. More broadly, convenience yields on assets may change with the state of the economy, and estimating no-arbitrage term-structure models allows us to learn how this is so.

The measurement in this paper has limitations for short-greenia due to scarcity of bonds issued at very short maturities. Green bonds, nonetheless, are typically issued at longer maturities for longer-term projects. Our measurement strategy can be extended for a more diverse set of issuers and a richer structure, allowing, for example, the measurement of green specific green bond default risk apart from convenience yields. More generally, measuring risk in green debt can inform both sovereign issuance strategy and the design of sustainable finance instruments for cost-effective climate finance.

References

- Ang, Andrew and Monika Piazzesi (2003) "A no-arbitrage vector autoregression of term structure dynamics with macroeconomic and latent variables," *Journal of Monetary Economics*, 50 (4), 745–787.
- Aron-Dine, Shifrah, Johannes Beutel, Monika Piazzesi, and Martin Schneider (2024) "Household climate finance: Theory and survey data on safe and risky green assets," Technical report, National Bureau of Economic Research.
- Baker, Malcolm, Daniel Bergstresser, George Serafeim, and Jeffrey Wurgler (2018) "Financing the response to climate change: The pricing and ownership of US green bonds," Technical report, National Bureau of Economic Research.
- Bauer, Michael D, Eric A Offner, and Glenn D Rudebusch (2025) "Green stocks and monetary policy shocks: Evidence from Europe," *European Economic Review*, 105044.
- Bauer, Michael D, Glenn D Rudebusch, and Jing Cynthia Wu (2012) "Correcting estimation bias in dynamic term structure models," *Journal of Business & Economic Statistics*, 30 (3), 454–467.
- Berk, Jonathan B and Jules H Van Binsbergen (2025) "The impact of impact investing," *Journal of Financial Economics*, 164, 103972.
- Bolton, Patrick and Marcin Kacperczyk (2021) "Do investors care about carbon risk?" *Journal of financial economics*, 142 (2), 517–549.
- Bretscher, Lorenzo, Alex Hsu, and Andrea Tamoni (2020) "Fiscal policy driven bond risk premia," *Journal of Financial Economics*, 138 (1), 53–73.
- Cao, Jie, Amit Goyal, Xintong Zhan, and Weiming Elaine Zhang (2024) "Unlocking ESG premium from options," *Swiss Finance Institute Research Paper* (21-39).
- Caramichael, John and Andreas C Rapp (2024) "The green corporate bond issuance premium," *Journal of Banking & Finance*, 162, 107126.
- Cheng, Gong, Eric Jondeau, and Benoît Mojon (2022) "Building portfolios of sovereign securities with decreasing carbon footprints," *Swiss Finance Institute Research Paper* (22-66).
- Chikhani, Pauline and Jean-Paul Renne (2025) "An analytical framework to price long-dated climate-exposed assets," Available at SSRN 3881262.
- Chittaro, Lautaro, Monika Piazzesi, Martin Schneider, and Marcelo Sena (2025) "Asset Returns as Carbon Taxes."

- Cochrane, John H and Jesus Saa-Requejo (2000) "Beyond arbitrage: Good-deal asset price bounds in incomplete markets," *Journal of political economy*, 108 (1), 79–119.
- Collin-Dufresne, Pierre, Robert S Goldstein, and Christopher S Jones (2008) "Identification of maximal affine term structure models," *The Journal of Finance*, 63 (2), 743–795.
- D'Amico, Stefania, Johannes Klausmann, and N Aaron Pancost (2023) "The benchmark greenium," Available at SSRN 4128109.
- Du, Wenxin, Benjamin Hébert, and Wenhao Li (2023) "Intermediary balance sheets and the treasury yield curve," *Journal of Financial Economics*, 150 (3), 103722.
- Duffie, Darrell and Rui Kan (1996) "A yield-factor model of interest rates," *Mathematical finance*, 6 (4), 379–406.
- Engle, Robert F, Stefano Giglio, Bryan Kelly, Heebum Lee, and Johannes Stroebel (2020) "Hedging climate change news," *The Review of Financial Studies*, 33 (3), 1184–1216.
- Fatica, Serena, Roberto Panzica, and Michela Rancan (2021) "The pricing of green bonds: are financial institutions special?" *Journal of Financial Stability*, 54, 100873.
- Flammer, Caroline (2021) "Corporate green bonds," *Journal of financial economics*, 142 (2), 499–516.
- Gabaix, Xavier (2007) "Linearity-generating processes: A modelling tool yielding closed forms for asset prices."
- (2012) "Variable rare disasters: An exactly solved framework for ten puzzles in macro-finance," *The Quarterly journal of economics*, 127 (2), 645–700.
- Giglio, Stefano, Bryan Kelly, and Johannes Stroebel (2021) "Climate finance," *Annual review of financial economics*, 13 (1), 15–36.
- Gormsen, Niels Joachim, Kilian Huber, and Sangmin Oh (2024) "Climate capitalists," Technical report, National Bureau of Economic Research.
- Hall, Robert E (1988) "Intertemporal substitution in consumption," *Journal of political economy*, 96 (2), 339–357.
- Hamilton, James D and Jing Cynthia Wu (2012) "Identification and estimation of Gaussian affine term structure models," *Journal of Econometrics*, 168 (2), 315–331.
- He, Zhiguo, Stefan Nagel, and Zhaogang Song (2022) "Treasury inconvenience yields during the COVID-19 crisis," *Journal of Financial Economics*, 143 (1), 57–79.

- Heinkel, Robert, Alan Kraus, and Josef Zechner (2001) "The effect of green investment on corporate behavior," *Journal of financial and quantitative analysis*, 36 (4), 431–449.
- Hong, Harrison and Marcin Kacperczyk (2009) "The price of sin: The effects of social norms on markets," *Journal of financial economics*, 93 (1), 15–36.
- Hong, Harrison, Jeffrey D Kubik, and Edward P Shore (2025) "Renewable Asset Price Volatility and Its Implications for Decarbonization," Technical report, National Bureau of Economic Research.
- Hong, Harrison and Edward Shore (2023) "Corporate social responsibility," *Annual Review of Financial Economics*, 15 (1), 327–350.
- Ilhan, Emirhan, Zacharias Sautner, and Grigory Vilkov (2021) "Carbon tail risk," *The Review of Financial Studies*, 34 (3), 1540–1571.
- Jiang, Zhengyang, Hanno Lustig, Stijn Van Nieuwerburgh, and Mindy Z Xiaolan (2024) "The US public debt valuation puzzle," *Econometrica*, 92 (4), 1309–1347.
- Joslin, Scott, Kenneth J Singleton, and Haoxiang Zhu (2011) "A new perspective on Gaussian dynamic term structure models," *The Review of Financial Studies*, 24 (3), 926–970.
- Klingler, Sven and Suresh Sundaresan (2023) "Diminishing Treasury convenience premiums: Effects of dealers' excess demand and balance sheet constraints," *Journal of Monetary Economics*, 135, 55–69.
- Kölbl, Julian F and Adrien-Paul Lambillon (2022) "Who pays for sustainability? An analysis of sustainability-linked bonds," *Swiss Finance Institute Research Paper*, 23.
- Krishnamurthy, Arvind and Annette Vissing-Jorgensen (2012) "The aggregate demand for treasury debt," *Journal of Political Economy*, 120 (2), 233–267.
- Larcker, David F and Edward M Watts (2020) "Where's the greenium?" *Journal of Accounting and Economics*, 69 (2-3), 101312.
- Li, Xicheng, Don Noh, Sangmin S Oh, Sean Seunghun Shin, and Jihong Song (2025) "Green Price Pressure," Technical report, Working Paper, HKUST.
- Lucas, Robert E, Jr (2000) "Inflation and welfare," *Econometrica*, 68 (2), 247–274.
- Nagel, Stefan (2016) "The liquidity premium of near-money assets," *The Quarterly Journal of Economics*, 131 (4), 1927–1971.

- Pástor, L'uboš, Robert F Stambaugh, and Lucian A Taylor (2021) "Sustainable investing in equilibrium," *Journal of financial economics*, 142 (2), 550–571.
- (2022) "Dissecting green returns," *Journal of financial economics*, 146 (2), 403–424.
- Pedersen, Lasse Heje (2025) "Carbon pricing versus green finance," *Journal of Finance*.
- Pedersen, Lasse Heje, Shaun Fitzgibbons, and Lukasz Pomorski (2021) "Responsible investing: The ESG-efficient frontier," *Journal of financial economics*, 142 (2), 572–597.
- Poggensee, Jannis (2025) "Generating shareholder value through the announcement of sustainability-linked bond issuance," *Journal of Climate Finance*, 10, 100057.
- Roch, Francisco, Sakai Ando, Chenxu Fu, and Ursula Wiriadinata (2023) "How Large is the Sovereign Greenium?" Available at SSRN 4427184.
- Sauzet, Maxime (2024) "Green intermediary asset pricing."
- Sauzet, Maxime and Olivier David Zerbib (2022) "When green investors are green consumers," in *Proceedings of the EUROFIDAI-ESSEC Paris December Finance Meeting*.
- Sidrauski, Miguel (1969) "Rational choice and patterns of growth," *Journal of Political Economy*, 77 (4, Part 2), 575–585.
- Zerbib, Olivier David (2019) "The effect of pro-environmental preferences on bond prices: Evidence from green bonds," *Journal of banking & finance*, 98, 39–60.

A. Data

A.1. Chilean sovereign green and sustainability bonds

This subsection documents the Chilean sovereign bonds in our dataset that are tagged as green or sustainability. These are use-of-proceeds instruments: an amount equal to net proceeds is allocated to eligible budget expenditures under Chile's sovereign green or sustainable financing framework. We report core contractual and framework information.

ISIN	US168863DL94
Bond tag (type)	Green (sovereign use-of-proceeds)
Currency	USD
Total issuance in USD	2,318,357,000
Issue date	2019-06-25
Maturity date	2050-01-25
Eligible use-of-proceeds (issuer)	Clean transportation; Energy efficiency; Renewable energy; Living natural resources, land use and marine protected areas; Efficient and climate-resilient water management; Green buildings

Table 6: Chilean sovereign green/sustainability bond summary for ISIN US168863DL94.

ISIN	US168863DN50
Bond tag (type)	Green (sovereign use-of-proceeds)
Currency	USD
Total issuance in USD	1,500,000,000
Issue date	2020-01-27
Maturity date	2032-01-27
Eligible use-of-proceeds (issuer)	Clean transportation; Energy efficiency; Renewable energy; Living natural resources, land use and marine protected areas; Water management; Green buildings

Table 7: Chilean sovereign green/sustainability bond summary for ISIN US168863DN50.

ISIN	US168863DV76
Bond tag (type)	Sustainability (sovereign use-of-proceeds)
Currency	USD
Total issuance in USD	1,500,000,000
Issue date	2022-01-31
Maturity date	2034-01-31
Eligible use-of-proceeds (issuer)	Access to essential health services; Access to basic housing; Access to education; Clean transport; Community support through job creation; Energy efficiency; Food security; Green buildings; Living natural resources, land use and marine protected areas; Renewable energy; Support for human rights victims; Support for low-income families; Support for the elderly or people with special needs; Water management

Table 8: Chilean sovereign green/sustainability bond summary for ISIN US168863DV76.

ISIN	US168863DW59
Bond tag (type)	Sustainability (sovereign use-of-proceeds)
Currency	USD
Total issuance in USD	1,000,000,000
Issue date	2022-01-31
Maturity date	2052-01-31
Eligible use-of-proceeds (issuer)	Access to essential health services; Access to basic housing; Access to education; Clean transport; Community support through job creation; Energy efficiency; Food security; Green buildings; Living natural resources, land use and marine protected areas; Renewable energy; Support for human rights victims; Support for low-income families; Support for the elderly or people with special needs; Water management

Table 9: Chilean sovereign green/sustainability bond summary for ISIN US168863DW59.

ISIN	US168863DX33
Bond tag (type)	Sustainability (sovereign use-of-proceeds)
Currency	USD
Total issuance in USD	1,500,000,000
Issue date	2022-01-31
Maturity date	2027-01-31
Eligible use-of-proceeds (issuer)	Access to essential health services; Access to basic housing; Access to education; Clean transport; Community support through job creation; Energy efficiency; Food security; Green buildings; Living natural resources, land use and marine protected areas; Renewable energy; Support for human rights victims; Support for low-income families; Support for the elderly or people with special needs; Water management

Table 10: Chilean sovereign green/sustainability bond summary for ISIN US168863DX33.

B. Asset Pricing Appendix

B.1. Model Fit

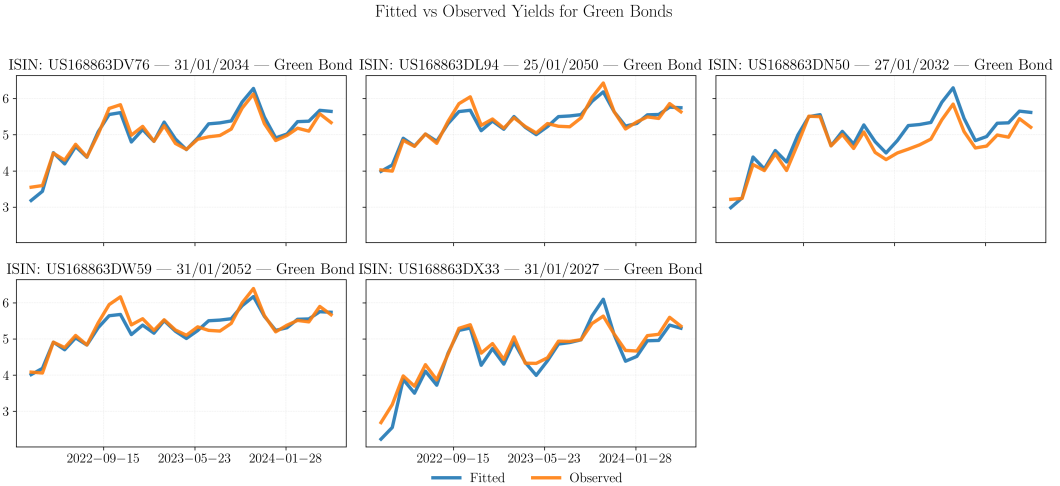


Figure 14: Model fit for green bonds: observed versus model-implied yields by maturity over time.

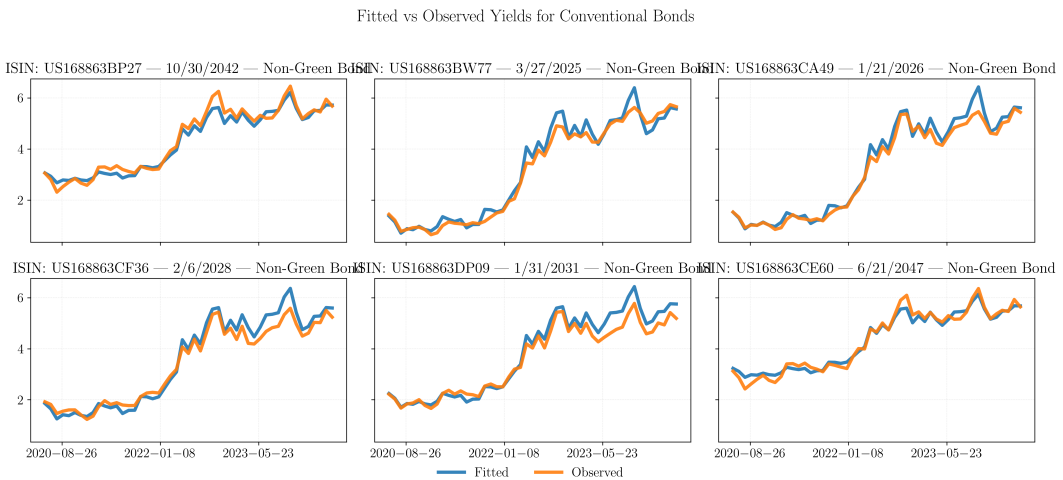


Figure 15: Model fit for conventional bonds: observed versus model-implied yields by maturity over time.

B.2. Pricing Equations

Here we specify the pricing equations implied by the exponentially affine model, making explicit the cross-equation restrictions across bonds and maturities implied by no-arbitrage. Prices are log-linear in the state vector.

For simplicity, we drop the j subscript indexing the bond type $\{G, C\}$, but it will become clear that the pricing equations are identical up to the short-rate parameters (ρ_0^j, ρ_1^j) and price of risk parameters $(\Lambda_0^j, \Lambda_1^j)$. Recall the exponentially affine model specification

$$z_t = \Psi z_{t-1} + \Sigma \varepsilon_{t+1} \quad (17)$$

$$M_{t+1} = \exp(-r_t - \frac{1}{2}\Lambda'_t \Lambda_t - \Lambda'_t \varepsilon_{t+1}) \quad (18)$$

$$\Lambda_t = \Lambda_0 + \Lambda'_1 z_t \quad (19)$$

$$r_t = \rho_0 + \rho'_1 z_t \quad (20)$$

The price of a coupon bond P_t that pays a stream of deterministic cash-flows $\{c_s\}_{s \geq t}$ is given by

$$P_t = \mathbb{E}_t \left[\sum_{s \geq t} M_s c_s \right] \quad (21)$$

$$= \sum_{s \geq t} P_t^{c_s} \quad (22)$$

where the second equality uses linearity of the expectation and defines the price of a coupon strip

$$P_t^{c_s} = \mathbb{E}_t [M_s c_s] \quad (23)$$

Equation (22) shows we can focus on the price of a coupon strip, since then to price the coupon bond we can sum over the prices of the strips. The derivation of the price of a coupon strip c_s is then identical to the derivation of the price of a zero-coupon bond. We can assume without loss of generality that the coupon at maturity pays 1, since

$$P_t^{c_s} = \mathbb{E}_t [M_s c_s] \quad (24)$$

$$= c_s \mathbb{E}_t [M_s] \quad (25)$$

$$= c_s P_t^s \quad (26)$$

where P_t^s is the price of a zero-coupon bond that pays 1 at maturity s .

Let $P_t^{(n)}$ be the price of a zero-coupon bond that pays 1 at date $t + n$. Guess that the price is log-linear in the state vector, i.e.,

$$\log P_t^{(n)} = A(n) + B(n)' z_t \quad (27)$$

Applying this guess to the right-hand side of the pricing equation (24)

$$P_t^{(n)} = \mathbb{E}_t \left[M_{t+1} P_{t+1}^{(n-1)} \right] \quad (28)$$

$$= \mathbb{E}_t \left[\exp \left(-r_t - \frac{1}{2} \Lambda'_t \Lambda_t - \Lambda'_t \varepsilon_{t+1} \right) \exp (A(n-1) + B(n-1)' z_{t+1}) \right] \quad (29)$$

$$= \mathbb{E}_t \left[\exp \left(-r_t - \frac{1}{2} \Lambda'_t \Lambda_t - \Lambda'_t \varepsilon_{t+1} \right) \exp (A(n-1) + B(n-1)' \{\Psi z_t + \Sigma \varepsilon_{t+1}\}) \right] \quad (30)$$

$$= \mathbb{E}_t \left[\exp \left(-r_t - \frac{1}{2} \Lambda'_t \Lambda_t - \Lambda'_t \varepsilon_{t+1} + A(n-1) + B(n-1)' \{\Psi z_t + \Sigma \varepsilon_{t+1}\} \right) \right] \quad (31)$$

$$= \exp \left(-r_t - \frac{1}{2} \Lambda'_t \Lambda_t + A(n-1) + B(n-1)' \Psi z_t \right) \mathbb{E}_t [\exp (-\Lambda'_t \varepsilon_{t+1} + B(n-1)' \Sigma \varepsilon_{t+1})] \quad (32)$$

$$= \exp \left(-r_t - \frac{1}{2} \Lambda'_t \Lambda_t + A(n-1) + B(n-1)' \Psi z_t \right) \mathbb{E}_t [\exp ((-\Lambda'_t + B(n-1)' \Sigma) \varepsilon_{t+1})] \quad (33)$$

$$= \exp \left(-r_t - \frac{1}{2} \Lambda'_t \Lambda_t + A(n-1) + B(n-1)' \Psi z_t \right) \exp \left(\frac{1}{2} \Lambda'_t \Lambda_t + B(n-1)' \Sigma \Lambda_t + \frac{1}{2} B(n-1)' \Sigma B(n-1)' \right) \quad (34)$$

$$= \exp \left(-r_t + A(n-1) + B(n-1)' \Psi z_t + B(n-1)' \Sigma \Lambda_t + \frac{1}{2} B(n-1)' \Sigma B(n-1)' \right) \quad (35)$$

$$= \exp \left(-\rho_0 - \rho'_1 z_t + A(n-1) + B(n-1)' \Psi z_t + B(n-1)' \Sigma \Lambda_0 + B(n-1)' \Sigma \Lambda_1 z_t + \frac{1}{2} B(n-1)' \Sigma B(n-1)' \right) \quad (36)$$

where the equality (34) uses the log-normality of $\exp((-\Lambda'_t + B(n-1)' \Sigma) \varepsilon_{t+1})$.

From the last equality and using the conjecture (27) in the left-hand side, we have

$$\exp(A(n) + B(n)' z_t) = \exp \left(-\rho_0 - \rho'_1 z_t + A(n-1) + B(n-1)' \Psi z_t + B(n-1)' \Sigma \Lambda_0 + B(n-1)' \Sigma \Lambda_1 z_t + \frac{1}{2} B(n-1)' \Sigma B(n-1)' \right) \quad (37)$$

$$\implies A(n) + B(n)' z_t = -\rho_0 - \rho'_1 z_t + A(n-1) + B(n-1)' \Psi z_t + B(n-1)' \Sigma \Lambda_0 + B(n-1)' \Sigma \Lambda_1 z_t + \frac{1}{2} B(n-1)' \Sigma B(n-1)' \quad (38)$$

The conjecture (27) is correct as long as equality (37) and (38) hold. Matching coefficients on z_t and the constants, this is true if and only if

$$A(n) = -\rho_0 + A(n-1) + B(n-1)' \Sigma \Lambda_0 + \frac{1}{2} B(n-1)' \Sigma B(n-1)' \quad (39)$$

$$B(n)' = -\rho'_1 + B(n-1)' \Psi + B(n-1)' \Sigma \Lambda_1 \quad (40)$$

Equations (39) and (40) are a system of difference equations that must be satisfied and yield the coefficients of the log-linear pricing equation. The boundary conditions that determine the solution are given by the condition that at maturity the price of the coupon strip is 1:

$$A(0) = 0 \quad (41)$$

$$B(0)' = 0 \quad (42)$$

Zero-coupon yields for maturity n are calculated as

$$y_t^{(n)} = -\frac{1}{n} (A(n) + B(n)' z_t) \quad (43)$$

and we define

$$a(n) = -\frac{1}{n}A(n), b(n) = -\frac{1}{n}B(n)' \quad (44)$$

B.3. Estimates of Parameters

Table 11: Estimates of Parameters

(a) Estimates of Λ_0^j		(b) Estimates of Short-Rate Parameters ρ		
	Λ_0^G	Λ_0^C	$\rho_0^{(x12)}$	$\rho_{1,\text{Level}}$
Level	-0.12	-0.05		
Green Factor	-0.13	0.05		
(c) Estimates of Λ_1^G			(d) Estimates of Λ_1^C	
	Level	Green Factor	Level	Green Factor
Level	-3.01	0.00	-3.11	0.00
Green Factor	0.00	0.00	0.00	0.00

B.4. Alternative Specifications

We show here alternative specifications of the term-structure model. In particular, we show the robustness of the downward sloping greenium term-structure to different number and different choice of factors. Table 12 summarizes the results.

Nº green factors	Nº factors total	Average Fitting Error (bps)	Green Bond Fitting Error (bps)	Conventional Bond Fitting Error (bps)	Greenium Slope	Short-term greenium mean (bps)	Short-term greenium std (bps)
0	1	16.29	16	16	-1.8	63	64
0	2	18.12	19	17	-1.3	23	34
0	3	17.30	17	17	-1.8	30	18
1	2	15.92	15	17	-1.7	38	14
1	3	18.97	18	20	-2.6	66	6
2	4	21.38	22	21	-1.8	11	2
2	4	20.46	20	21	-1.4	4	18

40

Table 12: Alternative factor specifications for the exponentially affine term-structure model. For the non-green factors, we use the level, slope and curvature factors from the principal components of conventional bond yields, in this pecking order. For example, in the case without green factors and a total of two factors, we use the level and slope factors.

One could entertain many other combinatorial choices of factors, of which we do not report here since they typically lead to economically implausible estimated stochastic discount factors, which in particular, fit poorly both green and conventional yields.

C. Model Appendix

C.1. Computing Conditional Moments

Given our estimates and the exponentially affine structure, we can compute conditional moments analytically. We recall the stochastic discount factor notation

$$m_{t+1} = -\delta_0 - \delta'_1 z_t - \frac{1}{2} \Lambda'_t \Lambda_t - \Lambda'_t \varepsilon_{t+1} \quad (45)$$

$$m_{t+1}^g = -\delta_0^g - \delta_1^{g'} z_t - \frac{1}{2} \Lambda_t^{g'} \Lambda_t^g - \Lambda_t^{g'} \varepsilon_{t+1} \quad (46)$$

Define $\|\Lambda_t\|^2 = \Lambda'_t \Lambda_t$.

From this, we have

$$y_{t+1} = -(\delta_0^g - \delta_0) - (\delta_1^g - \delta_1)' z_t - \frac{1}{2} (\|\Lambda_t^g\|^2 - \|\Lambda_t\|^2) - (\Lambda_t^g - \Lambda_t)' \varepsilon_{t+1} \quad (47)$$

$$= -\delta_0^y - \delta_1^{y'} z_t - \frac{1}{2} (\|\Lambda_t^g\|^2 - \|\Lambda_t\|^2) - \Lambda_t^{y'} \varepsilon_{t+1} \quad (48)$$

$$= -\delta_0^y - \delta_1^{y'} z_t - \frac{1}{2} (\|\Lambda_t^y\|^2 + 2\Lambda'_t \Lambda_t^y) - \Lambda_t^{y'} \varepsilon_{t+1} \quad (49)$$

where the second line is definitional.

The short interest rate is

$$i_t^{(1)} = -E_t[m_{t+1}] - \frac{1}{2} Var_t(m_{t+1}) \quad (50)$$

$$= \delta_0 + \delta'_1 z_t + \frac{1}{2} \Lambda'_t \Lambda_t - \frac{1}{2} \Lambda'_t \Lambda_t \quad (51)$$

$$= \delta_0 + \delta'_1 z_t \quad (52)$$

The conditional expectation of the convenience term is

$$y_{t+2} = -\delta_0^y - \delta_1^{y'} z_{t+1} - \frac{1}{2} (\|\Lambda_{t+1}^g\|^2 - \|\Lambda_{t+1}\|^2) - \Lambda_{t+1}^{y'} \varepsilon_{t+2} \quad (53)$$

$$\implies E_{t+1}[y_{t+2}] = -\delta_0^y - \delta_1^{y'} z_{t+1} - \frac{1}{2} (\|\Lambda_{t+1}^g\|^2 - \|\Lambda_{t+1}\|^2) \quad (54)$$

$$E_t[y_{t+2}] = -\delta_0^y - \delta_1^{y'} \Psi z_t - \frac{1}{2} E_t[\|\Lambda_{t+1}^g\|^2 - \|\Lambda_{t+1}\|^2] \quad (55)$$

The conditional variance is

$$Var_{t+1}(y_{t+2}) = \Lambda_{t+1}^{y'} \Lambda_{t+1}^y \quad (56)$$

The conditional covariance with the SDF

$$\text{Cov}_{t+1}(m_{t+2}, y_{t+2}) = \text{Cov}_{t+1}(-\Lambda'_t \varepsilon_{t+2}, -\Lambda'_{t+1} \varepsilon_{t+2}) \quad (57)$$

$$= \Lambda'_{t+1} \Lambda^y_{t+1} \quad (58)$$

For the expected greenium we have

$$E_t[g_{t+1}^{(1)}] = E_t[y_{t+2}] + \frac{1}{2} E_t[\Lambda'_{t+1} \Lambda^y_{t+1}] + E_t[\Lambda'_{t+1} \Lambda^y_{t+1}] \quad (59)$$

$$= -\delta_0^y - \delta_1^y \Psi z_t - \frac{1}{2} E_t[\|\Lambda_{t+1}^g\|^2 - \|\Lambda_{t+1}\|^2] + \frac{1}{2} E_t[\Lambda'_{t+1} \Lambda^y_{t+1}] + E_t[\Lambda'_{t+1} \Lambda^y_{t+1}] \quad (60)$$

$$= -\delta_0^y - \delta_1^y \Psi z_t - \frac{1}{2} E_t[(\|\Lambda_{t+1}^y\|^2)] - E_t[\Lambda'_{t+1} \Lambda^y_{t+1}] + \frac{1}{2} E_t[\Lambda'_{t+1} \Lambda^y_{t+1}] + E_t[\Lambda'_{t+1} \Lambda^y_{t+1}] \quad (61)$$

$$= -\delta_0^y - \delta_1^y \Psi z_t \quad (62)$$

C.2. Greenium term-structure decomposition

Let $Q_t^{(h)}$ and $Q_{g,t}^{(h)}$ denote, respectively, the prices at time t of a non-green and a green zero-coupon bond with h periods to maturity. Let

$$m_{t+1} := \log M_{t+1}, \quad y_{t+1} := \log(1 + Y_{t+1}), \quad m_{t+1}^g := m_{t+1} + y_{t+1},$$

and write the green pricing recursion for $h \geq 2$ as

$$Q_{g,t}^{(h)} = \mathbb{E}_t \left[M_{t+1}(1 + Y_{t+1}) Q_{g,t+1}^{(h-1)} \right] = \mathbb{E}_t \left[\exp(m_{t+1} + y_{t+1}) Q_{g,t+1}^{(h-1)} \right]. \quad (63)$$

The non-green recursion is identical with $y \equiv 0$. Define yields and the greenium

$$i_t^{(h)} := -\frac{1}{h} \log Q_t^{(h)}, \quad i_{g,t}^{(h)} := -\frac{1}{h} \log Q_{g,t}^{(h)}, \quad g_t^{(h)} := i_t^{(h)} - i_{g,t}^{(h)}.$$

The one-period prices and greenium are

$$Q_t^{(1)} = \mathbb{E}_t[e^{m_{t+1}}], \quad Q_{g,t}^{(1)} = \mathbb{E}_t[e^{m_{t+1} + y_{t+1}}], \quad g_t^{(1)} = \mathbb{E}_t[y_{t+1}] + \frac{1}{2} \text{Var}_t(y_{t+1}) + \text{Cov}_t(m_{t+1}, y_{t+1}).$$

For $1 \leq a \leq b$ define

$$\bar{m}_{a:b} := \sum_{j=a}^b m_{t+j}, \quad \bar{y}_{a:b} := \sum_{j=a}^b y_{t+j}.$$

Lemma 1. For each $h \geq 1$,

$$Q_{g,t}^{(h)} = \mathbb{E}_t \left[\exp(\bar{m}_{1:h} + \bar{y}_{1:h}) \right], \quad Q_t^{(h)} = \mathbb{E}_t \left[\exp(\bar{m}_{1:h}) \right]. \quad (64)$$

Proof. For $h = 1$ the identities follow from the one-period formulas above. For $h \geq 2$, use (63)

and the tower property:

$$Q_{g,t}^{(h)} = \mathbb{E}_t \left[e^{m_{t+1} + y_{t+1}} \mathbb{E}_{t+1} \left[e^{\sum_{j=2}^h (m_{t+j} + y_{t+j})} \right] \right] = \mathbb{E}_t \left[e^{\sum_{j=1}^h (m_{t+j} + y_{t+j})} \right].$$

The non-green case is the same with $y \equiv 0$. \square

Proposition 1 (greenium term-structure). *For every integer $h \geq 1$,*

$$h g_t^{(h)} = \sum_{j=1}^h \mathbb{E}_t [y_{t+j}] + \frac{1}{2} \text{Var}_t \left(\sum_{j=1}^h y_{t+j} \right) + \text{Cov}_t \left(\sum_{j=1}^h m_{t+j}, \sum_{j=1}^h y_{t+j} \right). \quad (65)$$

Proof. By Lemma 1 and the log-normal moment formula, for any (conditionally) Gaussian X , $\mathbb{E}_t[e^X] = \exp\{\mathbb{E}_t[X] + \frac{1}{2} \text{Var}_t(X)\}$, we have

$$\begin{aligned} \log Q_{g,t}^{(h)} &= \mathbb{E}_t [\bar{m}_{1:h} + \bar{y}_{1:h}] + \frac{1}{2} \text{Var}_t(\bar{m}_{1:h} + \bar{y}_{1:h}), \\ \log Q_t^{(h)} &= \mathbb{E}_t [\bar{m}_{1:h}] + \frac{1}{2} \text{Var}_t(\bar{m}_{1:h}). \end{aligned}$$

Since $g_t^{(h)} = -(1/h) \log Q_t^{(h)} + (1/h) \log Q_{g,t}^{(h)}$, subtracting the two yields (65). \square